



The University of  
**Nottingham**

UNITED KINGDOM • CHINA • MALAYSIA

Development of a Glucose Sensitive  
Insulin Delivery PLGA Microparticle  
System

MOHAMAD HADID AMSHAH BIN DINO

Thesis submitted to the University of Nottingham in fulfilment of the  
requirements for the Degree of Master of Philosophy

2017

## ACKNOWLEDGEMENT

I am thankful first and foremost to God for giving me the opportunity of continuing my passion for research. He has been with me every step along the way for which I am eternally grateful for.

I would like to extend my thanks to my supervisor Professor Nashiru Billa of the School of Pharmacy at the University of Nottingham, Malaysia Campus. The door to Professor Nashiru Billa office was always open whenever I ran into a trouble spot or had a question about my research or writing. He consistently allowed this paper to be my own work, but steered me in the right the direction whenever he thought I needed it. I would also like to acknowledge Professor Khiew Poi Sim of the Engineering Foundation faculty at the University of Nottingham, Malaysia Campus as the second reader of this thesis, and I am gratefully indebted to him for his very valuable comments on this thesis.

My thanks also goes to my lab mates in the drug delivery group as well as all the lab technicians, the academic and non-academic staff in the School of Pharmacy University of Nottingham, Malaysia campus for the diverse ways you contributed to the success of this project is really appreciated.

Finally, I must express my very profound gratitude to my parents: Professor Dino Isa Amshah and Salina Abdul Samad, as well as to my significant other for providing me with unfailing support and continuous encouragement throughout my years of study and through the process of researching and writing this thesis. This accomplishment would not have been possible without them. Thank you.

Sincerely,

Mohamad Hadid Amshah Dino

## 1. ABSTRACT

This project details the investigation done to formulate insulin-loaded PLGA microparticles for responsive insulin delivery. The formulations are to be tested for glucose specificity as a function of particle porosity later on in the investigation. The glucose responsive characteristic of the PLGA microparticle was modulated via incorporation of 4-formylphenyl boronic acid (4-FPBA) through conjugation with chitosan. Boronic acid moieties present in 4-FPBA are known to be sensitive to diols, such as glucose and fructose and is used here to provide the glucose sensing characteristic of the PLGA microparticles while chitosan is used as the anchor and readily forms nano- and micro-particles through ionic gelation with a suitable cross-linkers. The conjugation of 4-FPBA and chitosan proceeded through the Schiff's base method through N-reductive alkylation. The conjugates were characterized using Fourier transform infrared spectroscopy (FTIR), differential scanning calorimetry (DSC) and field emission scanning electron microscope (FESEM) analysis to ascertain the extend of bonding of the conjugate. The double solvent evaporation method was used to formulate porous and non-porous formulation. The non-porous formulation was found to be stable, discrete with no agglomeration seen through SEM analyses. Porosity was induced in the microparticle formulation through the use of porogens. Through optimization, stable and porous PLGA microparticles were formulated by enhancing the pores formed via exposure to ethanolic- NaOH. The glucose absorption of the PLGA microparticle samples was successfully measured through an indirect method utilising curcumin to detect 4-FPBA content in the microparticle sample. It was found that the increase in surface area afforded by the porous PLGA microparticle caused more of the 4-FPBA tagged chitosan to be incorporated within particles which resulted in higher 4-FPBA

content readily available in the porous microparticle sample. The higher 4-FPBA content correlates to a higher glucose sensitivity for the porous PLGA microparticles as observed in the higher insulin release profile obtained when compared to the non-porous microparticles. Porosity plays a vital role in increasing the glucose responsivity of the microparticles as the porous microstructure exposes more 4-FPBA to glucose and hence enhance the reactivity, allowing more of the incorporated insulin to be release as a consequence.

## TABLE OF CONTENTS

Acknowledgement.....	ii
<b>1. Abstract .....</b>	<b>iii</b>
<b>1. Introduction .....</b>	<b>1</b>
2.1 Background .....	1
2.2 Literature Review .....	5
2.3 Aims and Objectives .....	14
<b>3 Conjugation of Phenylboronic acid to chitosan to produce glucose sensitive chitosan .....</b>	<b>15</b>
3.1 Introduction .....	15
3.2 Materials and Equipment .....	18
3.3 Methods .....	19
3.3.1 General protocol for synthesis of conjugated 4-formylphenylboronic acid (4-FPBA) and chitosan .....	19
3.3.2 Modified protocol for the synthesis of conjugated 4-formylphenylboronic acid and chitosan .....	22
3.3.3 Fourier transform infra-red analysis (FTIR).....	23
3.3.4 Differential scanning calorimetry (DSC) .....	23
3.3.5 Enthalpy calculations .....	24
3.3.6 Field Emission Scanning electron microscopy (FESEM) .....	24
3.4 Results and Discussion .....	25
3.4.1 Formulation of 4-FPBA- chitosan conjugate .....	25
3.4.2 FTIR Analyses.....	26
3.4.3 DSC Analyses.....	29
3.4.4 Enthalpy Calculations.....	36
3.4.5 FESEM Imaging.....	39
3.5 Summary .....	42
<b>4.0 Formulation of porous and non-porous PLGA MicroparticleS.....</b>	<b>43</b>
4.1 Introduction .....	43
4.2 Materials and Equipment .....	46
4.3 Methods .....	46
4.3.1 General protocols for formulation of porous and non-porous PLGA microparticles .....	46
4.3.2 Protocols to enhance porosity of particles .....	48
4.3.3 Characterisation of PLGA microparticles by FESEM analysis.....	48
4.3.4 Porosity Calculations.....	48
4.3.5 Fourier transform infra-red analysis (FTIR).....	49

4.4	Results and Discussion .....	50
4.4.1	Formulation of non-porous PLGA microparticles .....	50
4.4.2	Optimisation of porous PLGA microparticle.....	52
4.4.3	Porosity Calculations.....	57
4.4.4	FTIR analyses on chitosan incorporated PLGA microparticles .....	59
4.5	Summary .....	64
5.0	Glucose absorption BY PLGA microparticles .....	65
5.1	Introduction .....	65
5.2	Method .....	70
5.2.1	HPLC analysis for glucose adsorption.....	70
5.2.2	Yield analysis of the 4-FPBA conjugated chitosan PLGA microparticles	70
5.3	Results and Discussion .....	72
5.3.1	HPLC analysis of curcumin .....	72
5.3.2	Yield analyses .....	78
5.4	Summary .....	81
6.0	Encapsulation and release of insulin from modified chitosan coated plga microparticles .....	83
6.1	Introduction .....	83
6.2	Materials and Equipment .....	86
6.3	Methods .....	87
6.3.1	Formulation of insulin loaded PLGA microparticles.....	87
6.3.2	HPLC analyses for insulin standard solution.....	87
6.3.3	Determination of the encapsulation efficiencies of microparticles.....	88
6.3.4	<i>In vitro</i> insulin release studies.....	89
6.4	Results and Discussion .....	91
6.4.1	HPLC analysis of insulin standard solution .....	91
6.4.2	Encapsulation efficiencies of porous and non-porous insulin loaded PLGA microparticles.....	92
6.4.3	<i>In vitro</i> insulin release studies of PLGA microparticles.....	95
	.....	96
6.5	Summary .....	99
7.0	Conclusions and Future Work.....	100
8.0	References.....	103
9.0	Appendices.....	108
9.1	FTIR spectra for formulations F2, F4 and F6 compared to pure PBA and pure chitosan. ....	108

## LIST OF TABLES

<b>TABLE 1: FORMULATIONS FOR CONJUGATED 4-FPBA -CHITOSAN .....</b>	<b>19</b>
<b>TABLE 2: ADDITIONAL FORMULATION FOR CONJUGATED 4-FPBA -CHITOSAN .....</b>	<b>22</b>
<b>TABLE 3: OPTIMISATION OF FORMULATION FOR POROSITY OF PLGA MICROPARTICLES .....</b>	<b>54</b>
<b>TABLE 4: POROSITY VALUES FOR NON-POROUS AND POROUS PLGA MICROPARTICLES FORMULATIONS .....</b>	<b>58</b>
<b>TABLE 5: FORMULATIONS FOR CHITOSAN COATED PLGA MICROPARTICLES STUDIES .....</b>	<b>59</b>
<b>TABLE 6: YIELD OF 4-FPBA IN NON-POROUS AND POROUS PLGA MICROPARTICLES FORMULATIONS .....</b>	<b>79</b>

## LIST OF FIGURES

<b>FIGURE 1: REPEATING UNIT IN PLGA POLYMER MATRIX.....</b>	<b>5</b>
<b>FIGURE 2: CHEMICAL STRUCTURE OF CHITOSAN.....</b>	<b>9</b>
<b>FIGURE 3: OVERALL REACTION BETWEEN CHITOSAN AND 4-FORMYLPHENYLBORONIC ACID (4- FPBA) .....</b>	<b>25</b>
<b>FIGURE 4: FTIR SPECTRA OF FORMULATIONS F1 TO F4 WITH RESPECT TO PURE CHITOSAN FORMULATED FROM PROTOCOLS DESCRIBED IN 3.3.1.....</b>	<b>26</b>
<b>FIGURE 5: COMPARISON BETWEEN FTIR SPECTRA OF FORMULATIONS F1,F3, F5 AND F7 WITH RESPECT TO PURE CHITOSAN AND 4-FPBA .....</b>	<b>28</b>
<b>FIGURE 6: DSC THERMOGRAM OF PURE CHITOSAN .....</b>	<b>30</b>
<b>FIGURE 7: DSC THERMOGRAMS OF FORMULATIONS F1, F3, F5 AND F7 WITH RESPECT TO PURE CHITOSAN .....</b>	<b>31</b>
<b>FIGURE 8: DSC THERMOGRAM OF PURE 4-FORMYLPHENYL BORONIC ACID(4-FPBA) .....</b>	<b>33</b>
<b>FIGURE 9: DSC THERMOGRAMS OF F1, F3, F5 AND F7 WITH RESPECT TO CHITOSAN AND 4- FPBA.....</b>	<b>34</b>
<b>FIGURE 10: ENTHALPY CALCULATIONS OF FORMULATIONS F1 AND F3 .....</b>	<b>37</b>
<b>FIGURE 11: ENTHALPY CALCULATIONS OF FORMULATIONS F5 AND F7 .....</b>	<b>37</b>
<b>FIGURE 12: FESEM IMAGES OF FORMULATIONS F1 TO F7 .....</b>	<b>40</b>
<b>FIGURE 13: FESEM IMAGES OF NON-POROUS PLGA MICROPARTICLES WITH A REPRESENTING THE FESEM IMAGE TAKEN AT 2500 X MAGNIFICATION AND B AT 500 X MAGNIFICATION. .....</b>	<b>50</b>
<b>FIGURE 14: FESEM IMAGES OF POROUS PLGA MICROPARTICLES WITH A REPRESENTING THE FESEM IMAGE TAKEN AT 2500 X MAGNIFICATION AND B AT 500 X MAGNIFICATION...</b>	<b>53</b>

<b>FIGURE 15: THE FESEM IMAGES OF POROUS FORMULATIONS F1 TO F4 AT 2500X</b>	
<b>MAGNIFICATION .....</b>	<b>55</b>
<b>FIGURE 16: THE SEM IMAGES FOR POROUS FORMULATIONS F5 TO F7 AT 2500X</b>	
<b>MAGNIFICATION .....</b>	<b>56</b>
<b>FIGURE 17: FTIR SPECTRA OF CHITOSAN COATED FORMULATIONS WITH RESPECT TO</b>	
<b>UNCOATED PLGA MICROPARTICLES (MP), PURE UNMODIFIED CHITOSAN AND 4-FPBA-</b>	
<b>CHITOSAN CONJUGATES .....</b>	<b>61</b>
<b>FIGURE 18: OVERALL CONVERSION OF GLUCOSE TO DETECTABLE NADH BY REACTION WITH</b>	
<b>HEXOKINASE REAGENT .....</b>	<b>66</b>
<b>FIGURE 19: CHEMICAL STRUCTURE OF ROSOCYANINE COMPLEX .....</b>	<b>67</b>
<b>FIGURE 20: OVERALL REACTION BETWEEN 4-FPBA MODIFIED CHITOSAN COATED PLGA</b>	
<b>MICROPARTICLES AND CURCUMIN .....</b>	<b>68</b>
<b>FIGURE 21: CHROMATOGRAM OF CURCUMIN STANDARD SOLUTION 50 µG/ML .....</b>	<b>72</b>
<b>FIGURE 22: CALIBRATION CURVE FOR CURCUMIN STANDARD SOLUTION 0 - 50 µG/ML .....</b>	<b>73</b>
<b>FIGURE 23: CURCUMIN CONSUMPTION (%) OF NON-POROUS AND POROUS PLGA</b>	
<b>MICROPARTICLES .....</b>	<b>76</b>
<b>FIGURE 24: COLOR CHANGE EXHIBITED BY NON-POROUS PLGA MICROPARTICLE (F1) AND</b>	
<b>POROUS PLGA MICROPARTICLES (F2) UPON REACTION WITH CURCUMIN .....</b>	<b>77</b>
<b>FIGURE 25: CHROMATOGRAM OF INSULIN STANDARD SOLUTION 500 µG/ML .....</b>	<b>91</b>
<b>FIGURE 26: CALIBRATION CURVE FOR INSULIN STANDARD SOLUTION 0 - 500 µG/ML .....</b>	<b>92</b>
<b>FIGURE 27: ENCAPSULATION EFFICIENCY OF NON-POROUS AND POROUS PLGA MICROPARTICLE</b>	
<b>.....</b>	<b>93</b>
<b>FIGURE 28 : INSULIN RELEASE PROFILE FOR POROUS AND NON-POROUS PLGA MICROPARTICLE</b>	
<b>FORMULATIONS .....</b>	<b>96</b>
<b>FIGURE 29: GLUCOSE RESPONSE BEHAVIOR OF BORONIC ACID MOEITIES .....</b>	<b>98</b>

# 1. INTRODUCTION

## 2.1 Background

Hyperglycaemia otherwise known as *diabetes mellitus* is one of the most common metabolic disorder that has seen a rapid increased in patients numbers around the world in the last decade (Chakraborty *et al.* 2011). *Diabetes mellitus* is commonly categorised as ‘Type 1’ and ‘Type 2 cases’. Type 1 diabetes manifests when the patient suffers from a deficiency of insulin leading to high blood sugar levels. The insufficient levels of insulin produced by the pancreas in Type 1 cases are thought to be due to the destruction of insulin-producing beta cells of the islets of Langerhans by autoimmune responses (Owens *et al.* 2016). On the other hand, type 2 diabetes is due to disorders in both insulin resistance and secretion caused by defects in the insulin receptors on the cell membranes (Owens *et al.* 2016). Of the two, Type 2 cases are the more common with approximately 90% of people diagnosed with *diabetes mellitus* having this type of diabetes (American Diabetes Association 2013).

Patients living with type 2 diabetes specifically require constant monitoring of blood glucose level that is regulated through a regimented lifestyle which includes modified dietary sugar intake, regular physical exercise as well as insulin therapy in the form of subcutaneous administration of insulin (American Diabetes Association 2012). However, insulin therapy in this manner results in a number of disadvantages including hypoglycaemia whereby the level of glucose in the bloodstream drop below the normal level as well as obesity due to intensive therapy, insulin neuropathy which is characterised by acute severe distal limb pain and in rare cases, insulin presbyopia

whereby patient may be visually impaired (farsightedness) due to dependence on insulin therapy (Sharma *et al.* 2015). In addition and with particular importance to the present research pursuit is that current administration of insulin employ up to four subcutaneous injections per day, causing psychological distress to the patient and leading to poor patient compliance (Carino *et al.* 2000).

These aforementioned drawbacks provide a challenge to researchers for exploration of possibilities that may improve upon the existing conventional modes of delivery in order to improve the quality of life of sufferers. Significant research has already been done which focuses on alternative routes of administration such as oral and pulmonary as well as ways to reduce the number of injectable doses to mitigate the drawbacks associated with conventional insulin treatment. While development of oral insulin formulation shows promise, major constraints to this mode of delivery include both enzymatic and physical barriers (Carino *et al.* 2000). Insulin, being proteinous, is prone to degradation by gastric acidity and intestinal enzymes when administered orally which consequently substantially decreases the bioavailability of the total insulin administered (Lowman *et al.* 2016). In addition, the relatively short half-life coupled with the fragile nature of orally formulated insulin are additional barriers that need to be overcome in order for orally-administered insulin therapy to be viable (Sharma *et al.* 2015). As such, the development of a commercial orally-based insulin delivery system has remained elusive.

Recently however, there is an increased interest in the development of micro- and nanoparticle drug delivery systems since these can be engineered to address some of the aforementioned constraints. Thus, it is not surprising that the development alternative insulin delivery systems seem to be harnessed around this technology. The use of microparticle and nanoparticle for drug delivery applications provides numerous

advantages over conventional methods and depending on the route of administration may include increased efficacy tolerability due to fewer doses and lesser dose cargo from the delivery system specificity and therapeutic index of the analogous drug (Hall *et al.* 2007). These advantages can further be enhanced by modifying the surface of the drug loaded nanoparticle or microparticle by conjugation with specific moieties that impart either passive or active targeting of specific cells or tissue (Singh & Lillard Jr. 2009). In addition, nano- and microparticles provide alternative pathways to the delivery of partially water-soluble drugs in an effective manner as well as targeting drugs to specific regions of the gastrointestinal tract. Indeed, studies have shown that the increased surface area of the small particles is exceedingly effective for targeted drug delivery (Chiranjib *et al.* 2013). In terms of health and safety, materials used to construct nanoparticles or microparticles, have to be stable, biodegradable, non-toxic, non-inflammatory and be able to escape the reticuloendothelial system when injected internally (Kumari *et al.* 2010).

Recent studies have shown that numerous polymeric and micellar nanocarriers provide desirable biopharmaceutical and pharmacokinetic properties in regards to insulin (Sharma *et al.* 2015). Studies done indicate several nanocarriers formulations suitable for insulin delivery include poly(lactic-co-glycolic acid) (PLGA) nanoparticles, detran-insulin nanoparticles and solid lipid-insulin nanoparticles (Sharma *et al.* 2015). Thus, insulin incorporated into these micro- and nanocarriers for selective and targeted delivery may provide better therapeutic outcomes in the treatment of diabetic patients by eliminating some of the drawbacks associated with the conventional treatment. This forms the core basis of the present work, whereby we aim to develop a potential insulin-containing microparticle delivery system taking into account the nature of materials used, which in this case are biodegradable and biocompatible, but also to drive along the premise of

reduced dosing frequency and sensitivity. Put together, these would address head-on the aforementioned constrained associated with current mode of insulin delivery.

## 2.2 Literature Review

This study focuses on the formulation of porous and non-porous insulin-loaded PLGA microparticles that have been tuned for glucose specificity in insulin release. PLGA polymers are popular in controlled drug delivery due to their excellent biodegradability, favourable degradation characteristic and sustained drug release capability which can be controlled by varying the molecular weight or the lactide/glycolide ratio of the polymer (Hirenkumar & Siegel 2012). Figure 1 shows the repeating ester units within the PLGA polymer chain. PLGA is also an FDA approved biomaterial that undergoes biodegradation after ingestion forming lactic and glycolic acids which are classified as non-toxic substances (Hirenkumar & Siegel 2012). Biodegradation of PLGA occurs mainly through hydrolysis but conflicting reports also shows the enzymatic degradation may also play a role (Hirenkumar & Siegel 2012). The lactic acid produced from this degradation process enters the tricarboxylic acid cycle before being eliminated from the body as carbon dioxide and water (Crotts & Park 1998). Similarly, glycolic acid also enters the tricarboxylic acid cycle and is eliminated from the body as carbon dioxide and water or alternatively, can be excreted in the kidney (Crotts & Park 1998).

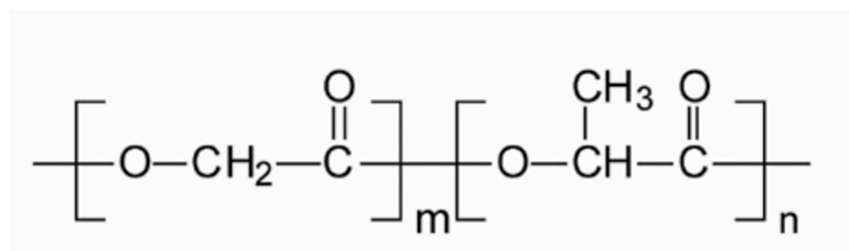


Figure 1: Repeating unit in PLGA polymer matrix

Polyester PLGA is regarded as the best defined biomaterial available for drug delivery with respect to design and performance (Birnbaum *et al.* 2000). This is due to the versatile nature of the polyester which can be processed into a wide variety of shapes and sizes as well as able to encapsulate molecules of varying molecular size (Hirenkumar & Siegel 2012). In addition, PLGA is soluble in a wide range of solvents including acetone, chlorinated solvents, and ethyl acetate among others which provides an advantage over other polymers during nanoparticle formulation (Birnbaum *et al.* 2000).

Documented studies have shown favourable data regarding the encapsulation of insulin PLGA nanoparticles. For example, Sun *et al.* (2010) prepared PLGA nanoparticles loaded with insulin-S.O (sodium oleate) complex via the double emulsion method to evaluate the pharmacological effects of oral administration to diabetic rats (Sun *et al.* 2010). The study found that the glucose levels in rats was reduced considerably after oral administration. In another study by Liu *et al.* (2007) insulin encapsulated PLGA nanoparticles were embedded into poly(vinyl alcohol) (PVA) hydrogels where, it was suggested that the composite system minimised the burst release of insulin from the nanoparticle, providing a more sustained release of the drug (Liu *et al.* 2007). In addition, numerous other studies conducted with insulin loaded PLGA nanoparticles are under-way to ascertain the potential advantages afforded by this polymer in oral based-drug delivery system (Zhang *et al.* 2012). These studies unequivocally show the potential of PLGA nanoparticles as an effective drug delivery system for insulin.

While PLGA particulates have been widely documented in drug delivery applications, there are potential drawbacks of utilising this polymer in targeted drug delivery. One drawback is that the surface charge of nano- microparticles particles from the polymer is slightly negative which limits the bioactivity when the nanoparticle interacts with the cell

membrane. This is because the cell membrane is also negatively charged and so can easily react more easily with more cationic particles to further facilitate endocytosis which is slightly hindered in the anionic polymer (Sharma *et al.* 2015). More importantly, due to the repeating ester units within the polymer chain whose activity is rather low (Figure 1), the surface of resulting particles tend to be passive and therefore active targeting of drug loaded PLGA nanoparticles is also difficult to achieve (Wang *et al.* 2013). This drawback has restricted the number of studies done with regards to targeted PLGA microparticles and nanoparticles in drug delivery applications unless some surface modification intervention is pursued. There have been a number of attempts to functionalise the surface of PLGA nanoparticles by coating with more reactive moieties (Guo & Gemeinhart 2008; Wang, Z *et al.* 2010; Wang, Y *et al.* 2013). Through this approach, the targeting capability of micro- and nanoparticles is possible.

Another widely used polymer in drug delivery applications is chitosan which can be found in shells of crustacean, the cuticles of insect and the cell wall of some fungi. Chitosan is composed of naturally occurring cationic polysaccharides and is the subject of many bioengineering applications as it is biodegradable and biocompatible as well as non-toxic (Ding *et al.* 2003). The chemical structure of chitosan is shown in figure 2. As with PLGA, chitosan can be formulated into tablets, microspheres, nanoparticles and membranes for drug delivery carriers (Sharma *et al.* 2015). In addition, chitosan can also be formulated to form films easily (Wang *et al.* 2013). Indeed, multiple studies have shown the viability of coating chitosan unto PLGA nanoparticles in an attempt to functionalise the surface of the nanoparticle (Guo & Gemeinhart 2008; Wang, Z *et al.* 2010; Wang, Y *et al.* 2013). For example, studies done by Wang *et al.* (2013) showed that the surface of PLGA nanoparticle drug delivery carrier can be functionalised by

coating with chitosan polymer (Wang *et al.* 2013). This was done by both physical desorption and chemical binding methods whereby the conventional double emulsion solvent evaporation method was modified slightly to incorporate chitosan into the formulation. The study concluded that PLGA modified by chitosan showed improved efficacy of 5-fluorouracil (5-FU) over non modified PLGA nanoparticles with a higher cumulative release of the drug in the same prolonged time (Wang *et al.* 2013). In another study by Wang *et al.* (2010), they formulated a tri-methylated chitosan-conjugated PLGA nanoparticle for the delivery of 6-coumarin across the blood-brain barrier (BBB) which further corroborated their previous result whereby the surface modified PLGA nanoparticle showed better efficacy of the loaded drug compared to non-modified PLGA nanoparticle (Wang *et al.* 2010). This change is brought about primarily due to the polycationic nature of chitosan which when coated upon the surface of the slightly negative surface charge on PLGA nanoparticle, causes the overall surface charge of the nanoparticle to be positive (Figure 2). As a consequence, there is increased interaction between the particles and the cell membrane which enhances the process of endocytosis (Sharma *et al.* 2015). Both studies and indeed most literature regarding chitosan coated PLGA nanoparticles show the versatility of the modified nanoparticle. The reactivity of microparticles was enhanced by coating with chitosan so that it was possible to conjugate specific moieties to the chitosan modified PLGA microparticles (Wang *et al.* 2013).

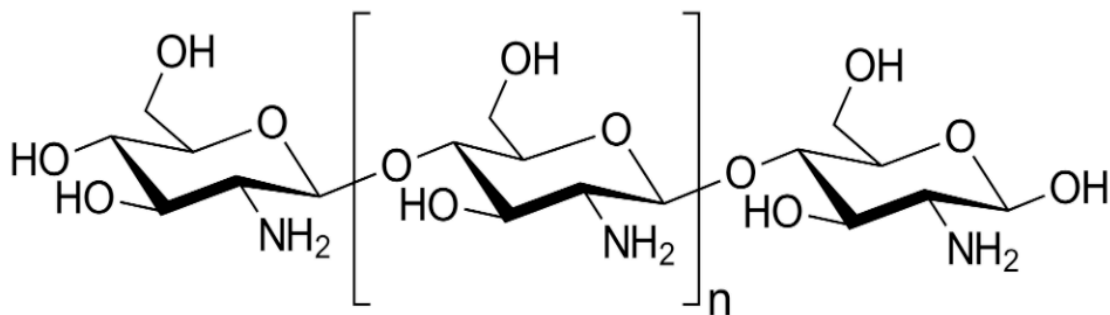


Figure 2: Chemical structure of chitosan

In the present study, glucose sensitivity was the desired objective and hence, the formulated PLGA microparticles requires moiety with this functionality. 4-formylphenylboronic acid (4-FPBA) which is documented to be sensitive to glucose absorption was conjugated to pure unmodified chitosan. Boronic acid and their derivatives have been used extensively in analytical and signalling chemistry as sensing diol moieties to detect glucose and is only just recently used in drug delivery applications specifically, in the formulation of glucose sensitive chitosan nanoparticles (Hall 2011; Siddiqui *et al.* 2017). In a related study to the present work, conjugation of 4-FPBA and chitosan was shown to be successful via a Schiff base through N-reductive alkylation of the amine groups in the chitosan backbone (Asantewaa *et al.* 2013; Siddiqui *et al.* 2017). In addition, the report also showed that the glucose absorption characteristic of 4-FPBA was relatively unhindered in the modified chitosan, except at very high boronic acid loading (Asantewaa *et al.* 2013). The conjugation of chitosan and boronic acid moieties is discussed in further detail in the next chapter. As in previous studies we report successful glucose sensitivity after conjugation of phenyl boronic acid with chitosan, and coating on PLGA microparticles.

Glucose sensitive phenylboronic acid (PBA) containing polymers shows promise in recent years due to its low cost, non-immunogenic and better in-vivo stability with a

range of glucose responsive material based upon PBA and its derivatives have been reported (Hall 2011). However, a major drawback of utilising these formulations in drug delivery is limited sustained drug release afforded with maximum period of only 2-5 days before additional application is required (Wu *et al.* 2017). On the other hand, PLGA based drug loaded nanoparticles and microparticles which offer a more sustained drug release profile as well as providing high loading capacity, encapsulation efficiency and favourable degradation characteristics provide an attractive co-polymer in PBA based glucose responsive drug delivery materials (Wu *et al.* 2017). The difficulty in functionalising the surface of the PLGA particle as mentioned previously forms a roadblock in forming these glucose sensitive PLGA microparticles, thus limiting the potential for glucose targeted PLGA microparticles. The novelty of this study is to provide an avenue to combine the properties of glucose responsivity in PBA based material and its derivatives with that of the versatile nature of PLGA based particulates through the use of chitosan coating. The relative ease of formulation through chitosan coating also provide an alternative to the more resource intensive controlled polymerization in order to instil targeting capability of PLGA micro- and nanoparticles. Another important aspect of the present study was to formulate both porous and non-porous insulin loaded microparticle in order to ascertain the influence of porosity on glucose sensitivity of the microparticles and hence insulin release. Presumably, porous microparticles are likely to offer an improvement in sensitivity to glucose due to the larger surface area compared to non-porous microparticles but the converse may also be true because of the likely leakiness of insulin from porous microparticles, which compromise on the cargo load (Arayne & Sultana 2006). Furthermore, slow release capability is possible from non-porous microparticles. The non-porous microparticles

also offer a large surface area due to the relatively smaller size dimension. Therefore, it is worth investigating to see how these two types of microparticles responds to external glucose concentrations. Hence, the main aim of the present proposal was to investigate how the surface area provided by the porosity from the porous microparticles as well as the smaller size dimension from the non-porous microparticles match-up with regards to sensitivity to glucose and hence insulin release. Previous studies based on a related theme show that porous nanoparticles manifested a faster but more sustained release of the analogous drug as compared to non-porous nanoparticles (Oh *et al.* 2011; Ilyas *et al.* 2013). Furthermore, investigations by Oh *et al.* (2011) on budesonide-loaded porous PLGA microparticles concluded that the percentage cumulative drug release was dependent upon the level of porosity of the particle (Oh *et al.* 2011). It must be added that the distinctive feature in the present proposal is that there is a trigger for drug (insulin) release, which adds to the mix of possibilities.

PLGA nanoparticles specifically benefits from porosity caused by accelerated polymer degradation from autocatalytic effects. When PLGA polymer is formulated into nanoparticles, the acids generated through hydrolytic reaction diffuses out of the particle. Furthermore, bases present in the bulk fluid diffuse into the nanoparticle, neutralising the acids. However, as the diffusional mass transport of these basses are relatively slow, the rate at which acids is generated within the nanoparticle can be much higher than the rate at which it is neutralized. Consequently, this leads to a decrease in the pH micro-environment within the particle (Siepmann *et al.* 2005). This in turn leads to an accelerated polymer degradation through autocatalysis which affects both drug mobility and release rate (Siepmann *et al.* 2005). In porous systems, the porosity of the particle

increases the diffusivity of water- soluble molecules from the polymeric matrices which reduces the autocatalytic effect (Fan & Singh 1989).

Studies by Ilyas *et al.* (2013) showed that an increase in size for drug loaded porous nanoparticles would result in a reduction in the relative release rates due to increase in length of diffusion pathways which decreases the rate of drug release to a more sustained profile (Ilyas *et al.* 2013). However, in the case of non-porous PLGA-based nanoparticle system, the increased diffusion pathway length effect is nullified due to autocatalysis effect resulting in unaltered drug release kinetics with increasing particle size (Klose *et al.* 2006). It can also be said that the pore characteristics have a significant impact on the underlying drug release mechanism as noted in a previous report whereby, porous PLGA nanoparticles showed better release behaviour due to the increase in available surface area for mass transfer (Arayne & Sultana 2006).

In the present study we focused on the formulation of microparticles which is defined as particulates having size range of approximately 2 to 2000  $\mu\text{m}$  (Singh *et al.* 2017). Microparticles formulated for drug delivery applications offer identical advantages to nanoparticles such as effective protection of the drug cargo from enzymatic degradation, encapsulation of water soluble drugs, appropriately tuned to accurately control the release rate of the cargo as well as instilling passive and active targeting capabilities (Singh *et al.* 2017). PLGA can be formulated to any size with relative ease and the preparation techniques are not too dissimilar from those of PLGA nanoparticles. Previously studies have shown that the double emulsion solvent evaporation method which is favoured for encapsulating hydrophilic drugs can be tuned to formulate either PLGA microparticles or nanoparticles by adjusting the disperse phase ratio and rate of stirring (Hirenkumar & Siegel 2012). This offers an avenue for fabrication of PLGA microparticles using

established protocols, whilst tuning relevant procedures in order to impart desirable characteristics such as porosity.

### **2.3 Aims and Objectives**

The overarching aim of the present investigation was to formulate porous and non-porous PLGA polymeric microparticles for the purpose of glucose stimulated insulin release.

The insulin loaded PLGA microparticles would be studied for glucose specificity and sensitivity with respect to porosity and size. Consequently, the following constitute the specific objectives for the study:

- I. Conjugation of boronic acid moiety (form of 4-formylphenylboronic acid (4-FPBA) to chitosan.
- II. The formulation of both porous and non-porous insulin loaded PLGA microparticles made from above conjugates.
- III. To compare the extent of sensitivity to glucose between the two types of microparticles.
- IV. Subsequently, to study the relationships between glucose sensitivity and porosity as a function of insulin release.

### 3 CONJUGATION OF PHENYLBORONIC ACID TO CHITOSAN TO PRODUCE GLUCOSE SENSITIVE CHITOSAN

#### **3.1 Introduction**

Recent developments on the capability of boronic-acid containing macromolecules has led to the advancement in key areas of biomedical applications such as saccharide sensing, controlled drug release and delivery of insulin, lipase inhibition as well as HIV inhibition to name a few (Fan & Singh 1989). Among these developments, significant attention has been given to the potential biological utility of boronic acid-conjugated polymers. These boronic acid- conjugated polymers are normally formulated into microgels or nanogels with specific properties such as thermal, glucose (saccharide), and pH responsiveness (Brooks & Sumerlin 2015). The degree or presence of these properties largely depend on the conjugated polymers chosen and can be tuned for a specific application as needed. For example, numerous studies on gels composed of 3-acrylamidophenylboronic acid (APBA) and N-isopropylacrylamide (NIPAM) showed remarkable synergistic combination of sugar and temperature sensitivity (Guan & Zhang 2013). In this case, sugar sensitivity is provided by the boronic acid moieties while the gel undergoes volume phase transition temperature inherent to the NIPAM co-polymer component (Guan & Zhang 2013). These properties designed for the hydrogels or microgels provide a strategy for applications in self-healing materials, drug delivery systems and saccharide sensors.

Most boronic acid conjugated polymers contain the phenylboronic acid (PBA) moieties component. An important characteristic of the boronic acid moieties is the ability of the

acid to form reversible complexes with 1,2 or 1,3 diols (Fan & Singh 1989). The formation of these complexes is due to the charged anionic tetrahedral form of the boronic acid in aqueous conditions which in the presence of a diol leads to stable boronate ester. Consequently, the conversion of neutral boronic acid moieties to anionic boronic ester causes the inherently hydrophobic property of boronic acid conjugated polymer to be more hydrophilic. This 'diol-responsive' behaviour of boronic acid is integral in formulating effective delivery strategies as most boronic acid conjugated polymer systems developed for insulin delivery rely upon this change in hydrophilicity in response to the presence of compatible diols (Fan & Singh 1989). Thus, boronic acid containing hydrogels such as chitosan combine the merits of both boronic acid and hydrogel (Brooks & Sumerlin 2015). Glucose responsivity is attained by the introduction of boronic acid while the swelling properties and three-dimensional network is provided by the polymer used.

Formulation of boronic acid conjugated polymers systems such as NIPAM occurs through controlled polymerization which is a resource intensive process that requires applications of heat and pressure to be successful (Brooks & Sumerlin 2015). Alternatively, with the use of chitosan polymer, boronic acid moieties can be directly linked to chitosan through reductive N-alkylation reaction of the reactive amine sites of the chitosan backbone (Smoum *et al.* 2006; Asantewaa *et al.* 2013). Essentially, the reaction is fairly similar to the reductive amination of aldehyde which involves the production of a carbinol amine which dehydrates to form an imine. The imine is then protonated utilizing an oxidising agent and subsequently reduction of this iminium ion ( $[R^1R^2C=NR^3R^4]^+$ ) produces the alkylated amine product which in this study, is the successfully conjugated chitosan. Utilising reductive N-alkylation is advantageous as the

reaction proceeds under mild conditions at a relatively fast rate of reaction (Abdel-Magid *et al.* 1996). Combined with the ability of chitosan to form films easily especially with slightly anionic polymers like PLGA, glucose responsive boronic acid conjugated polymers can be made with relative ease. In the present study we utilise 4-formylphenylboronic acid (4-FPBA) due to previous reports indicating successful conjugation with chitosan was achieved utilising the Schiff base method (Asantewaa *et al.* 2013; Siddiqui *et al.* 2017).

### **3.2 Materials and Equipment**

Low molecular weight chitosan (50 – 190 kda) was purchased from Sigma Aldrich (St.Louis, MO, USA); 4-formylphenylboronic acid (4-FPBA) and sodium borohydride were purchased from Thermo Fisher Scientific (Bridgewater, NJ, USA); pure acetic acid, methanol and ethanol were of reagent grade purchased from Thermo Fisher Scientific (Bridgewater, NJ, USA).

The equipment used were Perkin Elmer FTIR spectrometer (Spectrum RX1, PerkinElmer Ltd, United Kingdom) Field Emission scanning electron microscopy (FESEM) equipped with an Energy dispersive x –ray detector (EDX) (Model Quanta 400F, FEI Company, USA), Mettler Toledo TGA Differential Scanning Calorimetry (DSC) system (Mettler-Toledo (S) Pte Ltd, Singapore) and Beckman Benchtop Centrifuge (Allegra X-22R, Beckman Coulter, Inc., Indianapolis, USA).

### 3.3 Methods

#### 3.3.1 General protocol for synthesis of conjugated 4-formylphenylboronic acid (4-FPBA) and chitosan

The protocol used for the N-reductive alkylation of the amine group within the chitosan backbone to facilitate conjugation of chitosan with 4-FPBA is as follows: 50 mg of chitosan (0.3 mmol of NH<sub>2</sub>) was dissolved in 5 ml of 1% acetic acid and the mixture was stirred for 1 hour. The required amount 4-FPBA for each formulation as shown in Table 1 was dissolved in 15 ml methanol before being added into the chitosan solution. The mixture was stirred at 400 rpm using a magnetic stirrer for 1 hour under atmospheric pressure. The required amount of sodium borohydride (NaBH<sub>4</sub>) was added into the solution and continuously stirred for 24 hours at 300 rpm. After stirring, the mixture was poured into 50 ml centrifuge tubes. The precipitate was then collected by centrifugation for 10 minutes. The precipitate was washed with methanol, ethanol and water with centrifugation at 3 minute interval for each washing cycle. The samples were then frozen at -80 °C then freeze dried for 24 hours.

Table 1: Formulations for conjugated 4-FPBA -Chitosan

Formulation	Chitosan (mg)	Aldehyde Equivalent	4-FPBA (mg)	Sodium Borohydride (NaBH <sub>4</sub> ) (mg)
F1	50	1.5	67.5	27.2
F2	50	2.0	89.9	36.3
F3	50	2.5	112.4	45.4
F4	50	3.0	134.9	54.5

From Table 1, the amount of 4-FPBA required for each formulation was determined based upon the number of moles of NH<sub>2</sub> groups in chitosan (0.3 mmol of NH<sub>2</sub>) per 50

mg of chitosan (Smoum *et al.* 2006). By setting the aldehyde equivalent (moles of 4-FPBA) to be a multiple of the moles of  $\text{NH}_2$  group in the chitosan sample, the amount of 4-FPBA required for each sample can then be calculated. A sample calculation for F2 is shown in the following page. Furthermore, the amount of  $\text{NaBH}_4$  required for each formulation is equivalent to 1.6 times the moles of 4-FPBA added as per reports stating that successful conjugation of boronic acid to chitosan occurs when adequate amount of the oxidizing agent is present to precipitate the solid (Abdel-Magid *et al.* 1996).

## Sample Calculation for F2

For 4-FPBA,

50 mg of chitosan = 0.3 mmol of  $\text{NH}_2$  groups (based on literature)

For aldehyde equivalence of 2.0,

$$0.3 \times 2.0 = 0.6 \text{ mmol of aldehyde}$$

$$\text{MW of 4FPBA} = 149.90 \text{ gmol}^{-1}$$

From Elements of Chemical Reaction Engineering, Fourth Ed. (Fogler 2006),

$$n = \frac{\text{mass}}{\text{MW}}, \text{ mass} = n \times \text{MW} \dots\dots\dots (1)$$

$$\begin{aligned} \text{mass 4FPBA needed} &= 0.6 \text{ mmol} \times 149.90 \\ &= 89.9 \text{ mg} \end{aligned}$$

For Sodium Borohydride,

Literature reported need equivalent of 1.6 times the moles of the boronic acid added,

$$\begin{aligned} n_{\text{NaBH}_4} &= 0.6 \times 1.6 \\ &= 0.96 \text{ mmol} \end{aligned}$$

$$\text{MW of Sodium Borohydride} = 37.83 \text{ gmol}^{-1}$$

$$\begin{aligned} \text{Mass Sodium Borohydride required} &= 0.96 \text{ mmol} \times 37.83 \text{ mgmmol}^{-1} \\ &= 36.3 \text{ mg} \end{aligned}$$

### 3.3.2 Modified protocol for the synthesis of conjugated 4-formylphenylboronic acid and chitosan

It was found that the protocol presented in 3.3.1 did not yield a consistent trend over the four formulations studied. This is possibly due to insufficient amount of imine formation since the stirring after the addition of 4-FPBA into the chitosan solution only lasted for an hour. Subsequently, the protocol was modified as follows: firstly, the rate of stirring of the mixture containing chitosan and 4-FPBA in methanol was increased from 300 rpm to 800 rpm in order to speed up the reaction rate and the stirring time was extended to 3 hours. Previous studies reported successful reductive N-alkylation was accomplished by increasing the stirring time during imine formation (Abdel-Magid *et al.* 1996). Furthermore, the stirring time of the solution after addition of NaBH<sub>4</sub> was decreased to only 10 minutes as significant precipitate was observed upon immediate addition of NaBH<sub>4</sub> which is more in line with the other protocols reported.

Three additional formulations were studied with increased boronic acid content. Table 2 shows the additional formulations studied.

Table 2: Additional formulation for conjugated 4-FPBA -Chitosan

<b>Formulation</b>	<b>Chitosan (mg)</b>	<b>Aldehyde Equivalent</b>	<b>4-FPBA (mg)</b>	<b>Sodium Borohydride NaBH<sub>4</sub> (mg)</b>
<b>F5</b>	50	4.0	180.0	72.6
<b>F6</b>	50	8.0	360.0	145.3
<b>F7</b>	50	16.0	720.0	290.5

In order to ascertain the extent of conjugation of 4-formylphenylboronic acid to chitosan, a number of analytical techniques were employed including, Fourier transform infra- red (FTIR) spectroscopy, differential scanning calorimetry (DSC) thermogram, enthalpy calculations and field emission scanning electron microscopy (FESEM) imaging. Each of these techniques are described in details below.

### **3.3.3 Fourier transform infra-red analysis (FTIR)**

The FTIR spectra for all formulations as well as pure chitosan and pure 4-FPBA were obtained utilising a Perkin Elmer FTIR spectrometer. Prior to analysis, a small amount of the lyophilised sample was ground gently with approximately 250 mg of KBr powder until homogeneous powder was formed. The powder was then compressed under 6 tonnes of pressure (6000 psi) using a pneumatic table press to form a disc. The spectra were collected between 4000- 400  $\text{cm}^{-1}$ , with each measurement done in triplicates.

### **3.3.4 Differential scanning calorimetry (DSC)**

The thermograms were obtained from a TGA-Differential Scanning Calorimeter (DSC) equipped with a TGA Universal Analysis software<sup>®</sup>. Briefly, 5 to 10 mg of the sample was placed in a standard aluminium pan, covered with a lid and crimped using the crimping equipment. The pan with closed lid was then placed on to the DSC heating stage and heated from 0 to 400  $^{\circ}\text{C}$  at a constant heating rate of 10  $^{\circ}\text{C}/\text{min}$  and under a constant purge of nitrogen gas at 20 ml/min. The sample was heated along with an empty pan as a reference. The thermogram of pure chitosan and pure 4-FPBA was also obtained for comparison. The TGA Universal Analysis<sup>®</sup> software was used to compare each formulation with respect to the thermograms obtained from pure chitosan and 4-FPBA.

### **3.3.5 Enthalpy calculations**

The enthalpy ( $\Delta H$ ) at each melting episode for each formulation was obtained from TGA Universal Analysis software. The  $\Delta H$  is calculated from a typical DSC thermogram by integrating the area under the peak of the exothermic event.

### **3.3.6 Field Emission Scanning electron microscopy (FESEM)**

A small amount of the lyophilised sample was placed onto an FESEM imaging stub. The sample was then viewed under the FESEM at 10.0 kV.

### 3.4 Results and Discussion

#### 3.4.1 Formulation of 4-FPBA- chitosan conjugate

The conjugation of 4-FPBA and chitosan relies upon the Schiff's base whereby 4-FPBA was linked to chitosan through an N-reductive alkylation. This method is based upon a similar synthesis by Matsumoto *et al.* (2002) where researchers synthesised chitosan gel modified by phenylboronate for glucose absorption studies (Matsumoto *et al.* 2002). As mentioned earlier, this method involves the production of an imine intermediate which is further reduced to an amine upon addition of NaBH<sub>4</sub>. The overall reaction between chitosan and 4-FPBA through N-reductive alkylation reaction is shown in figure 3.

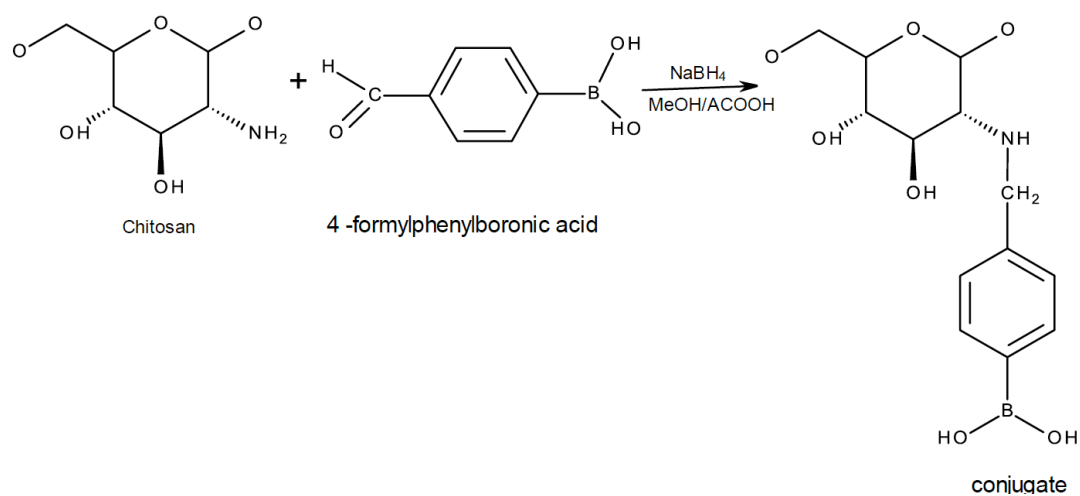


Figure 3: Overall reaction between chitosan and 4-formylphenylboronic acid (4-FPBA)

Studies done by Smoum *et al.* (2006) on the conjugation of PBA to chitosan showed that the degree of N-substitution was dependent upon the aldehyde equivalent that was added into the mixture (Smoum *et al.* 2006). Basically, conjugates with higher amount of boronic acid moieties can be formulated by simply increasing the amount of PBA in the reaction mixture.

### 3.4.2 FTIR Analyses

The FTIR spectra of the formulations were compared with pure chitosan to ascertain any observable trend by the increased level of the aldehyde equivalent in the mixture. In the first approach described in section 3.3.1, the four formulations did not show any noticeable trend across the four samples as shown in Figure 4.

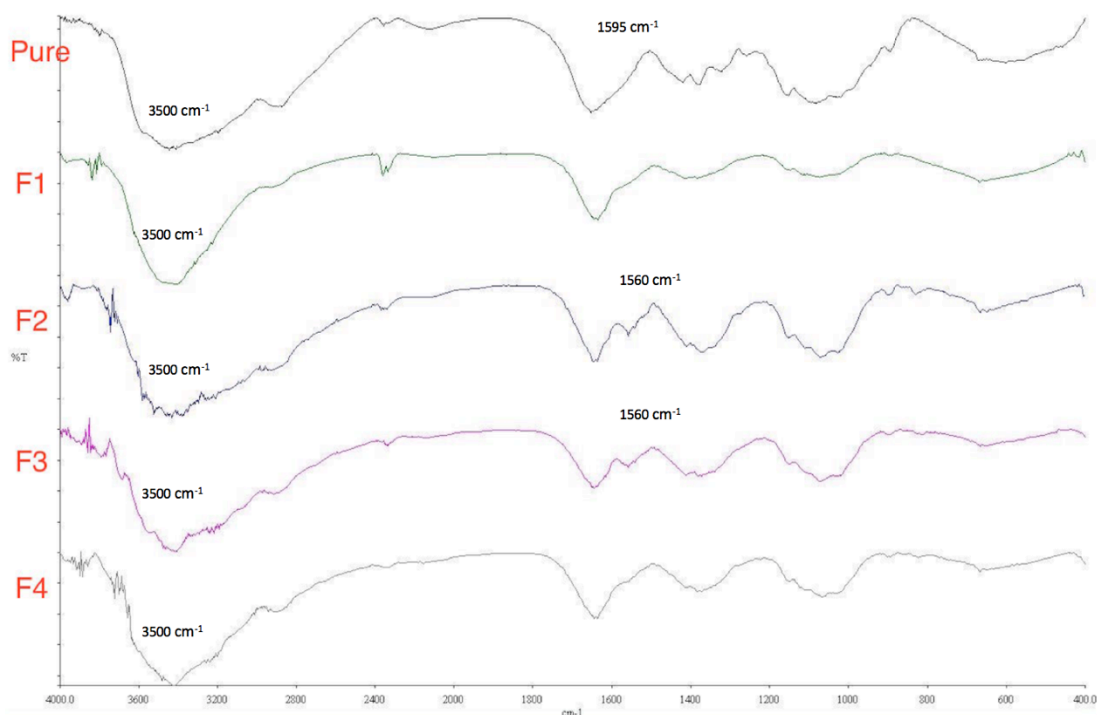


Figure 4: FTIR spectra of formulations F1 to F4 with respect to pure chitosan formulated from protocols described in 3.3.1

Notwithstanding, the characteristic peak for chitosan at  $3500\text{ cm}^{-1}$  corresponding to N-H bond stretching is seen in all formulations (Smoum *et al.* 2006). This is an important characteristic peak that may be used for identification once the chitosan-conjugated boronic acid is incorporated onto the PLGA microparticles. Further inspection shows that a clear peak is manifested at  $1595\text{ cm}^{-1}$  in the spectrum for pure chitosan corresponding

to the primary amine  $\text{NH}_2$  vibration deformation (Smoum *et al.* 2006). This is an indication of successful conjugation of 4-FPBA to chitosan and the peak should gradually disappear as the degree of N-substitution should increase with increase in 4-FPBA in subsequent formulations as reported in previous studies (Asantewaa *et al.* 2013; Smoum *et al.* 2006). However, from Figure 4, it can be seen that only F2 and F3 produced peaks at  $1560\text{ cm}^{-1}$  indicating the presence of substituted benzene, albeit minute intensity while also deemphasizing the primary amine peak. In contrast, F1 and F4 showed little to no observable changes compared to chitosan suggesting the conjugation was unsuccessful.

The formation of imine is a reversible reaction and therefore the rate of reaction is considerably slow and does not proceed to completion if the reaction time is inadequate (Abdel-Magid *et al.* 1996). Hence, once the oxidizing agent was added to the mixture after a relatively short stirring time, the precipitate collected was the modified chitosan that failed to undergo a full N-reductive alkylation reaction. This resulted in F1 and F4 having distinctly similar FTIR spectra with respect to pure unmodified chitosan as the boronic acid content in these conjugates were lower than expected. Thus, from the FTIR spectra produced from these four formulations, the conjugation of 4-FPBA to chitosan was deemed to be inconclusive. In this case, the stirring time of 1 hour and stirring speed of the mixture set at 300 rpm was recognized as the limiting factor.

Modifications of the protocols described in 3.3.2 incorporates a longer stirring time of 3 hours as well as increasing the stirring speed of the magnetic stirrer to 800 rpm to ensure the rate of reaction proceeds to completion and the formation of imine. The increase in stirring time has been reported to show better conjugation results (Abdel-Magid *et al.* 1996). In addition, 3 additional formulations were studied to accurately convey the trend observed through the FTIR analyses. The samples were then compared with pure 4-

FPBA as well as pure chitosan in order to fully characterize the differences between each formulation.

The FTIR spectra formulations F1, F3, F5 and F7 are shown in Figure 5 with respect to 4-FPBA and chitosan. The range of the spectra was adjusted to  $2000\text{ cm}^{-1}$  to  $400\text{ cm}^{-1}$  for ease of analysis. The FTIR spectra formulations F2, F4 and F6 are also shown in appendix 9.1.

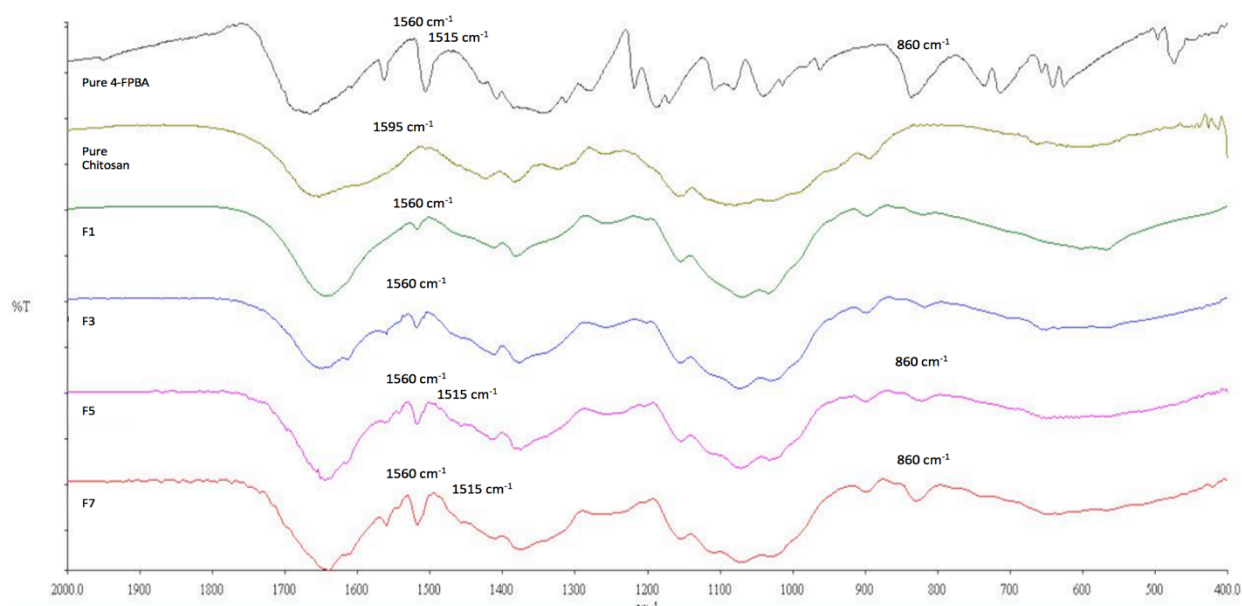


Figure 5: Comparison between FTIR spectra of formulations F1, F3, F5 and F7 with respect to pure chitosan and 4-FPBA

It can be seen in Figure 5 that the samples showed a more consistent trend than in the previous formulations (Figure 4). The characteristic peak corresponding to the primary amine of chitosan at  $1590\text{ cm}^{-1}$  was observed to be less apparent from F1 through F7 which suggest that 4-FPBA was successfully bonded to the primary amine site on the chitosan backbone. Further analysis of the spectra revealed that additional peaks were formed at  $1560\text{ cm}^{-1}$ ,  $1515\text{ cm}^{-1}$  and  $816\text{ cm}^{-1}$  which further resolved into sharper peaks

from F1 to F7. These peaks correspond to the absorption bands of the para substituted benzene and support the evidence that the conjugation was successful and was brought about through the N-reductive alkylation reaction of the primary amine (Smoum *et al.* 2006).

When compared with pure 4-FPBA, the peaks corresponding to the  $\rho$  - di- substituted benzene becomes sharper as the degree of N-substitution in the formulations were increased as seen in Figure 5. Indeed, the peaks of the samples starts to mimic those present in pure crystallised 4-FPBA specifically at  $1560\text{ cm}^{-1}$  and  $1515\text{ cm}^{-1}$  especially in F5 and F7. This shows that there is a direct correlation between the intensity of the peaks and the degree of substitution achieved in the formulations as the conjugates with the highest degree of substitution manifested the highest peak intensity.

From the FTIR spectra in Figure 5, it can be deduced that 4-FPBA has been successfully conjugated to chitosan through N-reductive alkylation. Comparisons with pure chitosan showed that the reactive site reside in the primary amine group as reported in several other studies (Asantewaa *et al.* 2013; Smoum *et al.* 2006). Comparison with pure 4-FPBA showed that as the aldehyde equivalent was increased in each subsequent formulation, more of the boronic acid moieties were able to undergo N-reductive alkylation with chitosan which resulted in a higher degree of substitution in the conjugates.

### 3.4.3 DSC Analyses

Differential scanning calorimetric (DSC) analyses were conducted in order to observe the physical changes brought about after the successful conjugation of 4-FPBA to chitosan. As the degree of substitution increased, the modified chitosan showed a change in

material organization thereby changing the physical properties of the material. By utilizing DSC, these changes can be discerned.

Figure 6 shows the DSC thermogram of pure chitosan. Chitosan was characterised by having two peaks, one endothermic peak and one exothermic peak. Similar result was reported by Kittur *et al.* (2002) on chitin, chitosan and their carboxymethyl derivatives (Kittur *et al.* 2002). The endothermic peak at 108 °C was due to the dehydration of water contained in the chitosan polymer (Ding *et al.* 2003). Furthermore, the exothermic peak at 315 °C was due the degradation of the chitosan main chain due to excess dehydration, thermal effects and de-polymerisation (Ding *et al.* 2003). More importantly, the degradation of the amine group (-NH<sub>2</sub>) in the chitosan backbone was also thought to occur at this peak (Asantewaa *et al.* 2013).

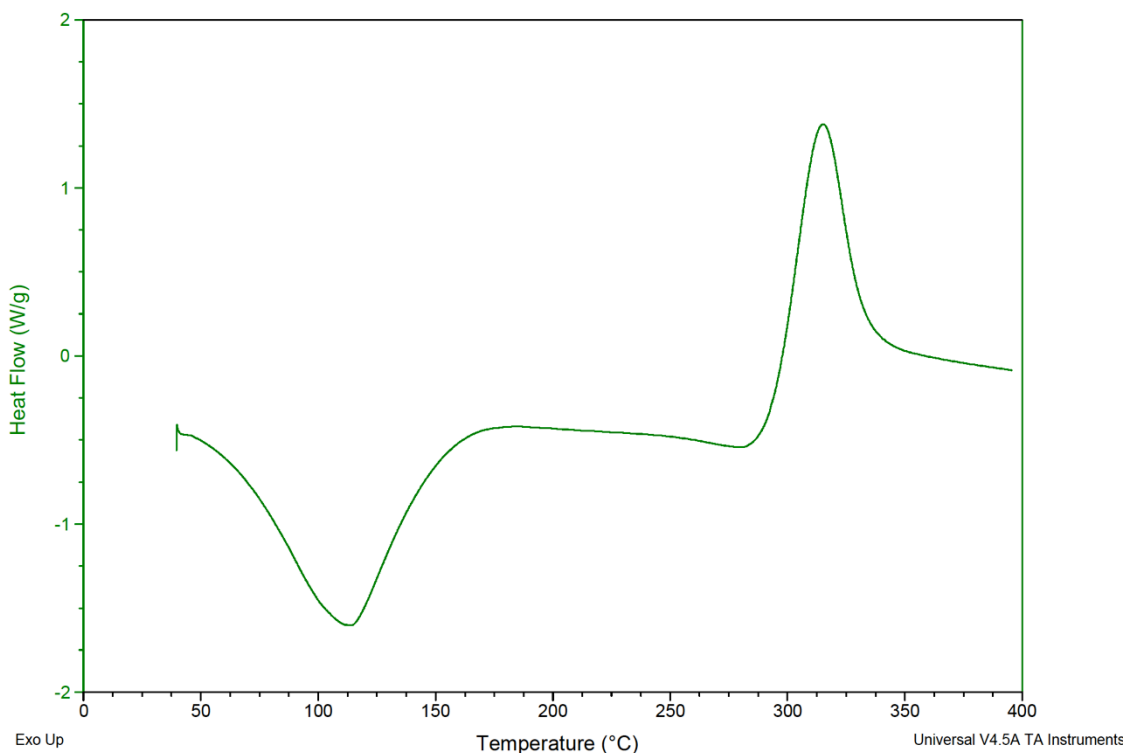


Figure 6: DSC thermogram of pure chitosan

The thermograms for the formulations F1, F3, F5 and F7 were compared to that of pure chitosan as shown in Figure 7. This was done to help discern any observable trend with each subsequent formulation.

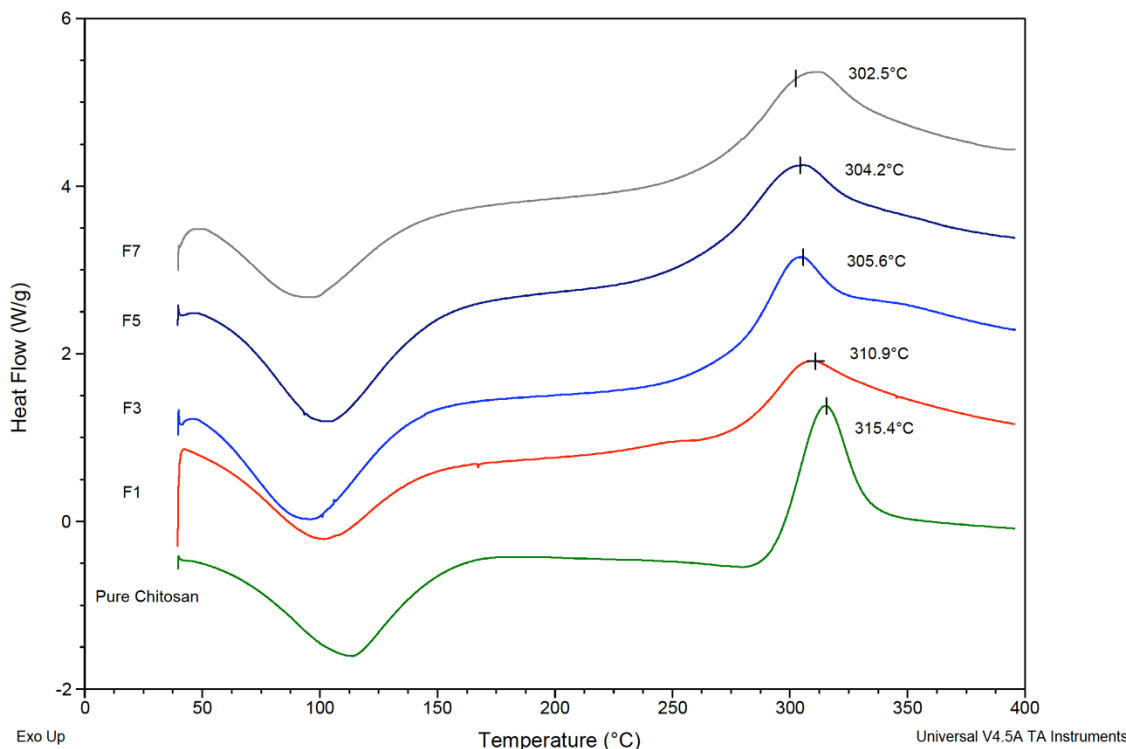


Figure 7: DSC thermograms of formulations F1, F3, F5 and F7 with respect to pure chitosan

From Figure 7, it can be seen that the samples exhibit an endothermic peak at approximately 100 °C which were slightly shifted to the left of the peak manifested in pure chitosan sample. Similar to that of unmodified chitosan, the endothermic peaks seen in the samples are due to the dehydration of water molecules from  $\text{-NH}_2$  and  $\text{-OH}$  groups in the chitosan backbone.

More importantly, it can be seen that the exothermic peaks of the conjugated chitosan were progressively shifted to the left with respect to the same exothermic peak produced from the pure chitosan. As this peak is correlated to the decomposition of  $\text{-NH}_2$  groups,

the reduction in decomposition temperature seen in the conjugates suggest that there was a consumption of  $-NH_2$  groups brought upon by the N-reductive alkylation reaction with increase in boronic acid content. Thus, the shift in decomposition temperature was correlated to an increase in degree of substitution. As the aldehyde equivalent was increased from F1 to F7, leading to an increased in the degree of substitution, it was observed that the decomposition temperature of the conjugates becomes lower with each subsequent formulation.

Along with pure chitosan, the conjugates were also compared with pure 4-FPBA. Determination of true melting point of boronic acid and their derivatives has historically been documented as difficult to characterise accurately (Hall 2011). Rather than true melting points, combustion analysis of boronic acids are more likely reflective of the dehydration and decomposition points (Hall 2011; Santucci & Gilman 1958). This is due to the inherent water content in the sample which affects the acid-anhydride transition, resulting in a range of melting points (Santucci & Gilman 1958). Figure 8 shows the DSC thermogram for pure 4-FPBA.

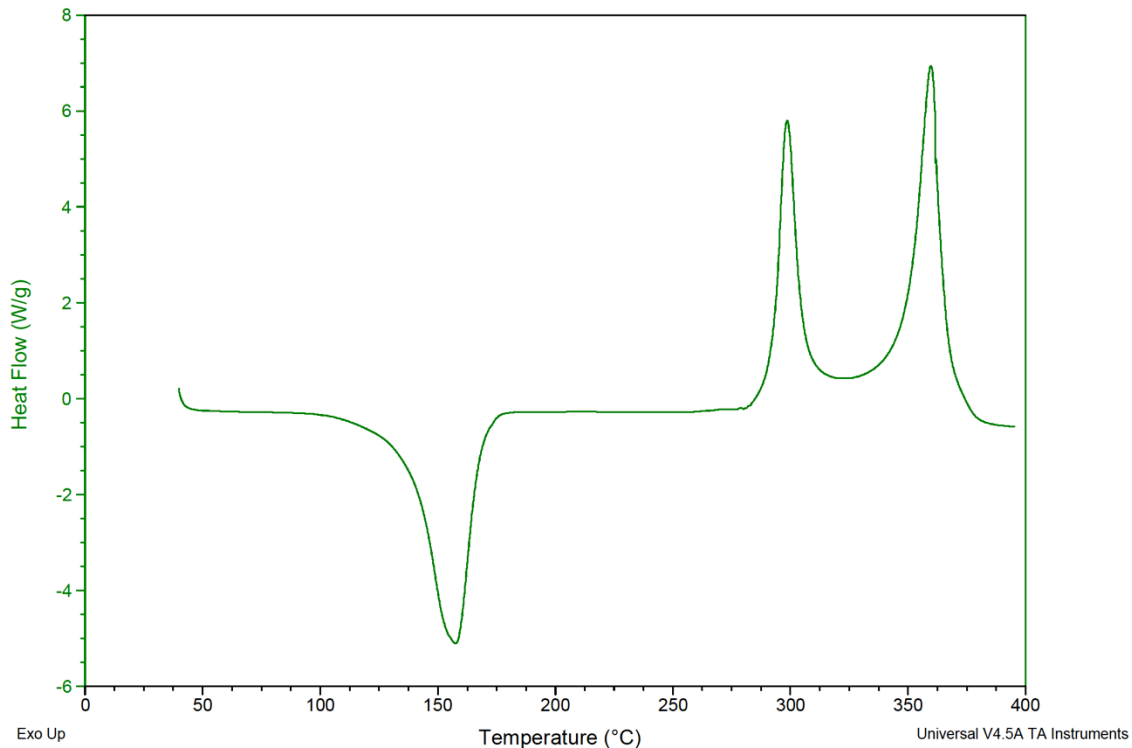


*Figure 8: DSC thermogram of pure 4-formylphenyl boronic acid (4-FPBA)*

From figure 8, it can be seen that the 4-FPBA sample for this study was characterised by 3 peaks with one endothermic peak and two exothermic peaks. The endothermic peak seen at 155 °C was primarily due to the dehydration of water molecules from the 4-FPBA sample. It was reported that the thermal dehydration of boronic acid leads to the formation of anhydride boronic acid known colloquially as boroxines (Hall 2011). Hence, the exothermic peak at 299 °C represents the re-solidification of the anhydride derivative produced from thermal dehydration while the second exothermic peak at 352 °C represents the melting point of this anhydride as previously reported by Santucci & Gilman (1958) in a study describing the decomposition of bromine and sulphur containing aromatic boronic acid (Santucci & Gilman 1958). It is worth noting that due to the facile dehydration of boronic acid, reproducibility of this result with 4-FPBA of

different purities is hard to achieve as those samples would have different water content and hence, variable heating rates are required to achieve similar results. Water content in 4-FPBA sample correlates with the purity of the product from the manufacture. In this study, 4-FPBA sample with an assay of 95% purity obtained from Sigma Aldrich is used for all formulations. This is a major reason most studies report on the melting point of the anhydride derivative of the boronic acid as it is more reliable (Hall 2011).

Figure 9 show comparisons between 4-FPBA and the conjugates (F1, F3, F5 and F7).

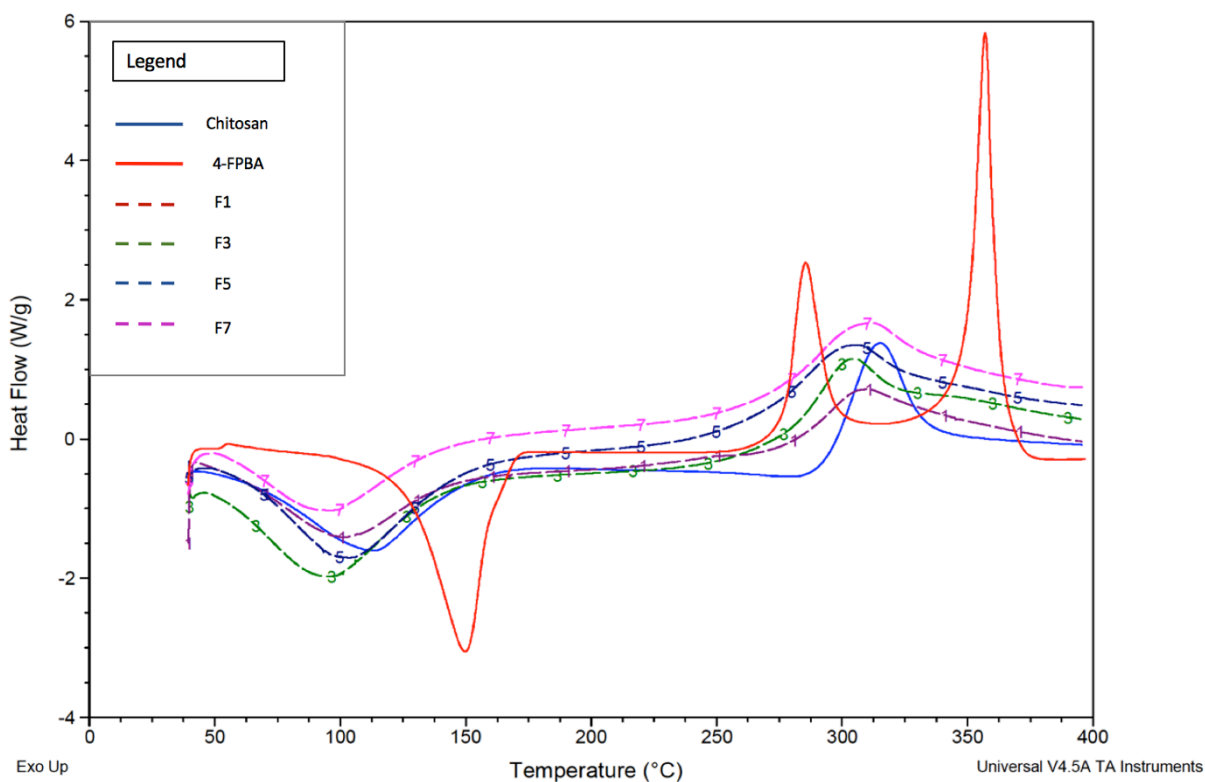


Figure 9: DSC thermograms of F1, F3, F5 and F7 with respect to chitosan and 4-FPBA.

Note: The formulations are presented as dotted lines and a number specifying the formulation. The solid blue line represents the DSC thermogram of chitosan while 4-formylphenylboronic acid(4-FPBA) is represented by the solid red line

As previously noted, the exothermic peak of the conjugates was shifted to the left of the peak from pure chitosan. However, in the present comparison, as the degree of substitution was increased from F1 to F7, the exothermic peak of the conjugates was observed to shift more towards the first exothermic peak of 4-FPBA (to the right). This result suggests higher degree of boronic acid substitution favours the formation of the anhydrous alternative.

Comparisons from the DSC thermograms produced by the conjugates reveal that the conjugation of 4-FPBA with chitosan resulted in the decomposition of  $-NH_2$  in the chitosan backbone as well as an increase in the formation of anhydrous boronic acid from F1 to F7. Thus, DSC analysis was successful in corroborating the results obtained from FTIR analysis as well as indicating that there was a change in physical property and consequently, in material organization of the conjugated samples.

#### 3.4.4 Enthalpy Calculations

The enthalpy change ( $\Delta H$ ), is calculated as the area under the exothermic peak in the DSC thermogram obtained. As reported by Kittur *et al.* (2002), an increase in  $\Delta H$  of the exothermic peak is directly related to the degree of substitution (Kittur *et al.* 2002). As the free unsubstituted amine group is involved directly in Schiff's base reaction, the  $\Delta H$  of the exothermic peak in the formulations can be used to ascertain the extent of the conjugation between 4-FPBA and chitosan. The  $\Delta H$  was calculated through the use of the integration by linear function in the TGA Universal Analysis software<sup>®</sup>. Figure 10 shows the enthalpy changes for formulation F1 and F3 whilst Figure 11 shows those for F5 and F7.

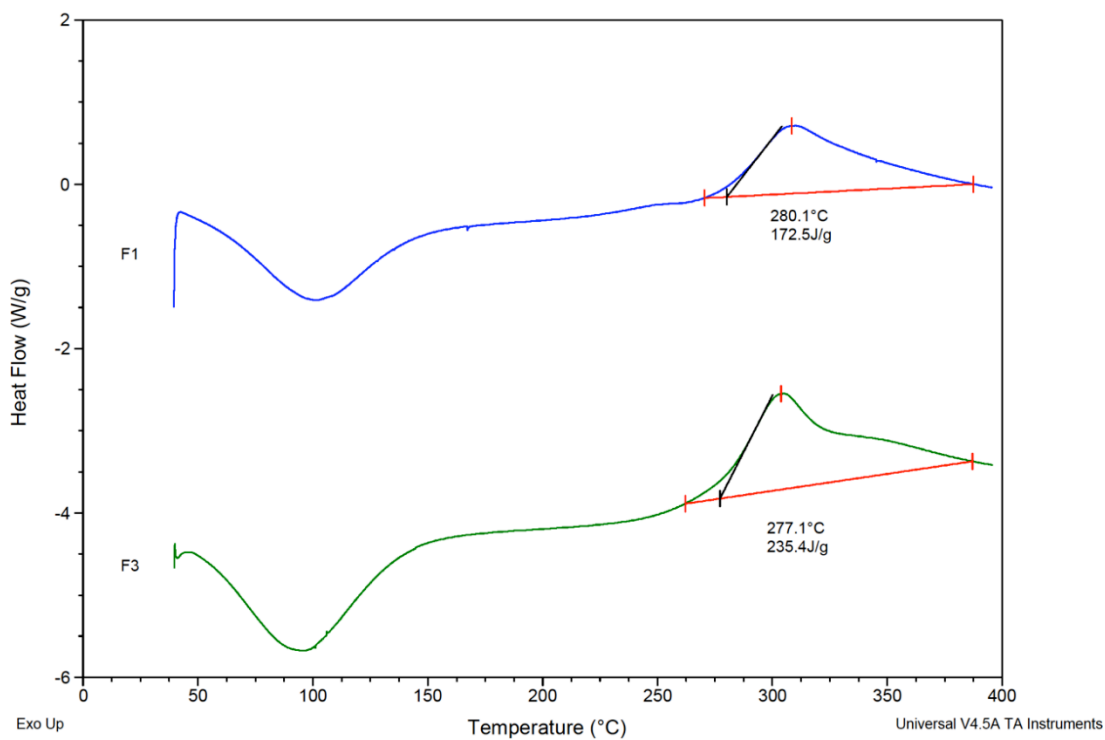


Figure 10: Enthalpy calculations of formulations F1 and F3

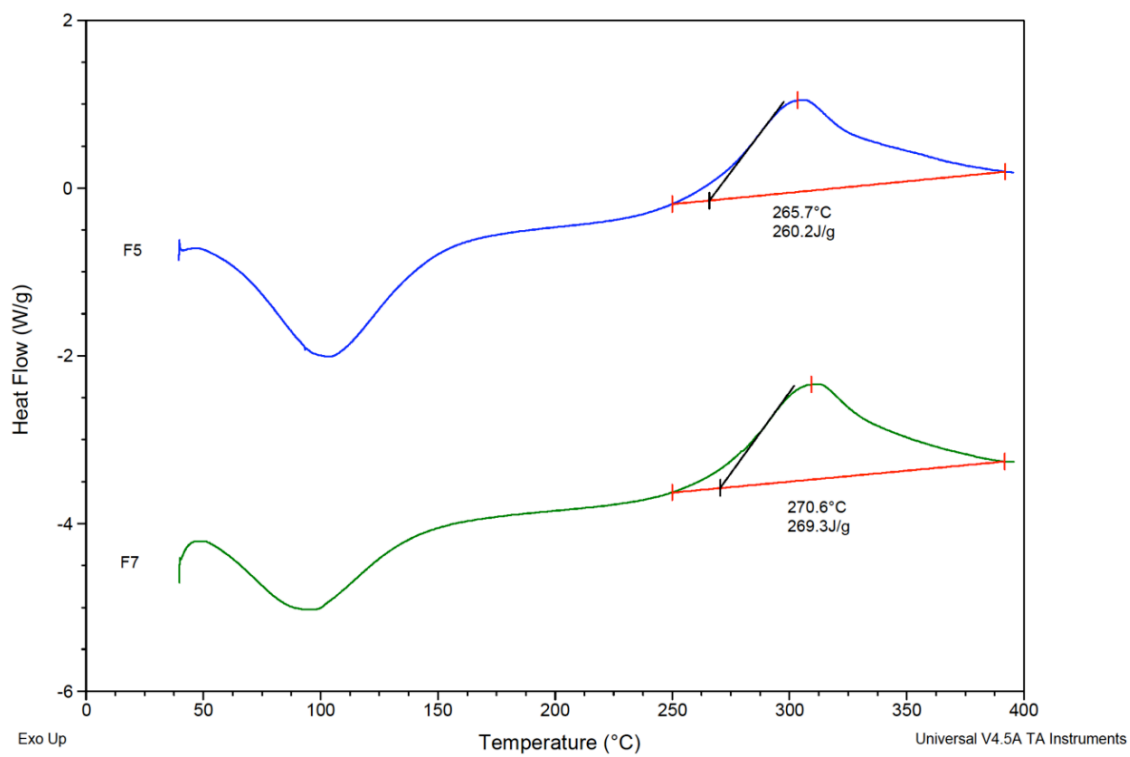
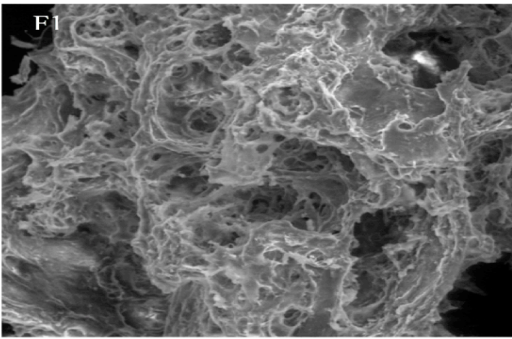


Figure 11: Enthalpy calculations of formulations F5 and F7

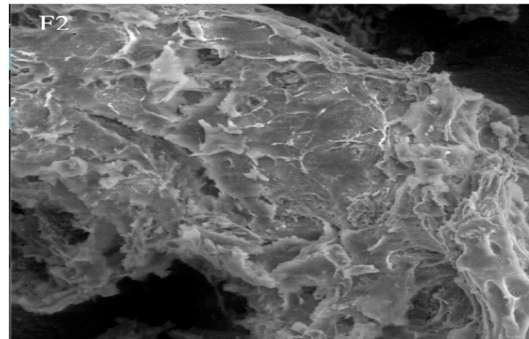
From both figures, it can be seen that the  $\Delta H$  values increased from F1 to F3 and again from F5 to F7 indicating that the chemical and molecular structure of the formulations were modified through the conjugation with 4-FPBA. 4-FPBA is known to be crystalline while chitosan is more amorphous so that with an increased level of substitution from F1 to F7, we should expect an increased level of crystallinity for the conjugates. Consequently, more heat was required to facilitate the decomposition of the more crystalline formulations which resulted in a higher  $\Delta H$  value reported. The effects of crystallinity were expanded further in the FESEM (discussed in the next page) analysis performed. Thus, this result supports both the findings in the FTIR and DSC analyses and confirms the successful bonding of 4-FPBA to chitosan.

### **3.4.5 FESEM Imaging**

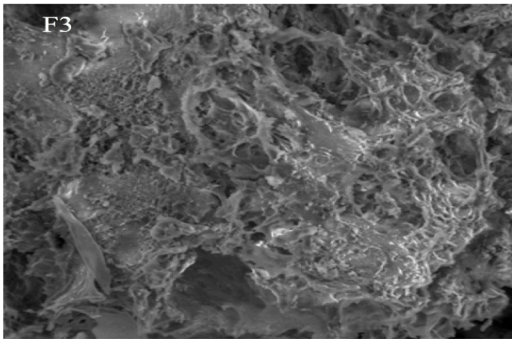
From the enthalpy analyses, it is expected that the molecular structure of the 4-FPBA conjugated chitosan was modified to the more crystalline conformation. The FESEM imaging was done to visually illustrate this physical change. Figure 12 shows captured SEM images for the formulations F1 to F7. The imaging was done at a magnification of 1200X at 10.0 kV.



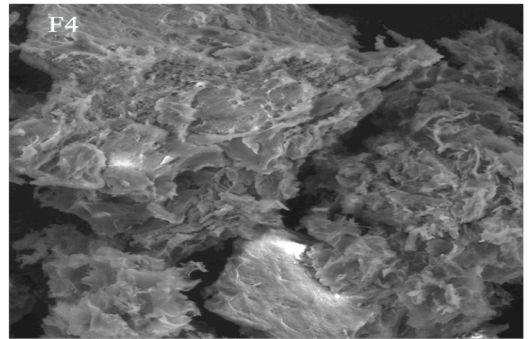
50  $\mu\text{m}$



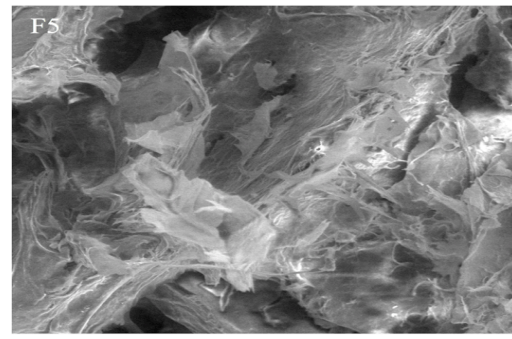
50  $\mu\text{m}$



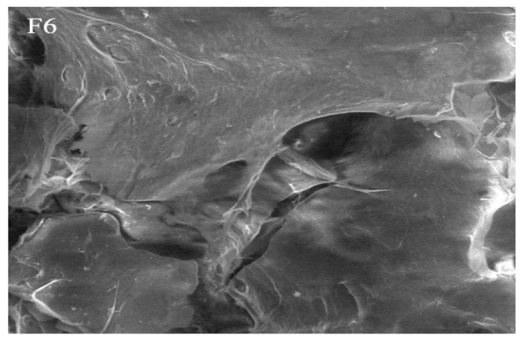
50  $\mu\text{m}$



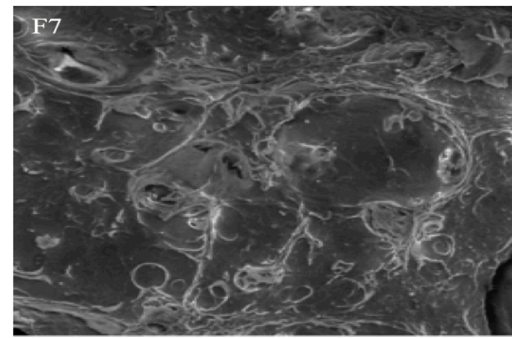
50  $\mu\text{m}$



50  $\mu\text{m}$



50  $\mu\text{m}$



50  $\mu\text{m}$

Figure 12: FESEM images of formulations F1 to F7

It can be observed from the FESEM images that the conjugates exhibited a more porous and spongy looking surface from F1 to F4. As the degrees of substitution in these conjugates are relatively low, the SEM images reflected the more amorphous structure of chitosan. However, the conjugates started to progressively show a flat hard surface from F5 to F7 indicative of a more crystalline structure. As 4-FPBA is inherently crystalline in structure, conjugates with high 4-FPBA content should better reflect this crystalline nature as observed (Asantewaa *et al.* 2013).

Polymer crystallinity are normally determined utilising DSC by quantifying the heat associated with the melting and decomposition of the polymer (Blaine 2015). This was done in the previous enthalpy analysis whereby there was an increase in  $\Delta H$  values from F1 to F7 suggesting a more crystalline structure in the later formulations. Thus, these FESEM images gives a visual representation of this increased in crystallinity of the conjugates and directly corroborates the results obtained from enthalpy analysis. Overall, both results strongly suggest that the increased in the degree of substitution in chitosan with 4-FPBA led to a more crystalline structure in the conjugates.

### 3.5 Summary

The results showed that the conjugation of 4-formylphenylboronic acid (4-FPBA) to chitosan was successful and proceed through N-reductive alkylation reaction by utilizing the Schiff's base method. From the FTIR spectra of the conjugates, it was found that the boronic acid moiety was bonded to the reactive primary amine site of the chitosan backbone. DSC analyses was then performed and the results showed that the material organisation of the conjugates was significantly altered by the conjugation. Comparison between the DSC thermograms of the conjugates with respect to pure chitosan revealed that an increase in the degree of substitution in the conjugates was correlated to the consumption of the  $-NH_2$  group thereby corroborating the results from FTIR analysis. Further comparison of the conjugates shows that the conjugates with high amount of boronic acid content tends towards emulating the physical properties of pure 4-FPBA more than that of pure chitosan suggesting the physical properties of the conjugates were modified through the addition of the boronic acid moieties.

The change in enthalpy ( $\Delta H$ ) confirmed that the physical properties of the conjugates gradually changes as the degree of substitution increases resulting in a different mechanism of chitosan decomposition. FESEM images revealed more insight in the physical changes of the conjugates. It was found that conjugates with lower degree of substitution showed a more porous and spongy surface similar to that of unmodified chitosan. However, conjugates with higher degree of substitution showed a flat surface suggesting a more crystalline structure similar to that of 4-FPBA.

## 4.0 FORMULATION OF POROUS AND NON-POROUS PLGA MICROPARTICLES

### 4.1 Introduction

In this chapter we focus on the preparation of porous and non-porous PLGA microparticles. In addition, the produced microparticles need to be coated by the boronic acid conjugated chitosan in order to impart the glucose sensing capability.

The general method used in preparing PLGA microparticles includes the creation of oil-in-water (O/W) and water-in-oil-in-water ( $W_1/O/W_2$ ) emulsions by utilizing high speed homogenisation and probe tip sonication. As insulin is hydrophilic, the more suitable method would be the water-in-oil-in-water ( $W_1/O/W_2$ ) otherwise known as the double emulsion method as it has become the more favoured approach for encapsulating hydrophilic compounds and protein (Hirenkumar & Siegel 2012). This double emulsion process involves first producing the water in oil phase (W/O) by initially dissolving an appropriate amount of drug in aqueous phase using deionized water. The aqueous phase ( $W_1$ ) is then added to an organic solution (O) containing the PLGA polymer and the chosen solvent such as dichloromethane (DCM), ethyl acetate (EA) or acetone yielding the water in oil phase ( $W_1/O$ ). The water in oil primary emulsion is then added to the chosen surfactant solution ( $W_2$ ) such as polyvinyl alcohol (PVA) or Polysorbate 80, which is then further emulsified at an appropriate stress mixing conditions creating the double emulsion phase ( $W_1/O/W_2$ ). The organic solvent is then extracted through solvent evaporation to yield the microparticle which is then washed thoroughly and freeze dried.

Studies show that the choice of solvent, surfactant and stirring rate predominantly affects the drug encapsulation efficiency as well as the particle size (Birnbaum *et al.* 2000). The most popular surfactant used for drug loaded PLGA microparticle formation is PVA. Emulsification with PVA is known to form particles of relatively small size and uniform size distribution (Birnbaum *et al.* 2000; Sahoo *et al.* 2002). It is found that residual PVA cannot be completely removed from the particles and can be retained at high levels in the solution (up to 10% by mass) (Hirenkumar & Siegel 2012; Sahoo *et al.* 2002). Residual PVA is important in maintaining the hydrophilic nature of the microparticles after drying to ensure re-suspension of the nanoparticles in aqueous solution (Hirenkumar & Siegel 2012). In addition, a study by Sahoo *et al.* (2002) on the effect of residual PVA associated with physical and cellular uptake of PLGA nanoparticles observed that residual PVA influence the particle size, zeta potential, protein loading as well as the *in vitro* release of the encapsulated drug (Sahoo *et al.* 2002). Thus, these parameters can be easily tuned by altering the PVA concentration in the formulation. These advantages afforded by PVA makes it the most suitable choice of surfactant in this study.

There are a number of approaches reported for formulation of porous microparticles such as porogen leaching method, emulsion/freeze drying and expansion in supercritical fluid to name a few (Arayne & Sultana 2006). The porous microparticle produce can vary in size depending on the protocols, equipment and reagents used in each experiment. Therefore, an important consideration to induce porosity in microparticles must take into account the suitability of the method with the aims of the study. A popular method to formulate porous microparticles as viable drug carriers is by introducing porosity through the use of porogens. These porogens such as ammonium bicarbonate, phosphate buffer saline and hydrogen peroxide to name a few, can be incorporated directly into the double

emulsion solvent evaporation method to induce porosity (Qutachi *et al.* 2014). Addition of these porogens into the primary aqueous phase ( $W_1$ ) leads to a porous structure during rapid polymer precipitation (Luan *et al.* 2006). Phosphate buffer saline (PBS) was chosen in the present study for induction of porosity in the microparticles as it is capable in producing consistent pores in PLGA nanoparticles with potential for drug delivery (Qutachi *et al.* 2014).

The plan is to coat the formed porous and non-porous microparticles with the 4-FPBA conjugated chitosan in order to impart the glucose sensing capability. Numerous studies suggest that successful coating can be achieved by incorporating the chitosan in the second aqueous phase ( $W_2$ ) of the double emulsion solvent evaporation method (Wang, Z *et al.* 2010; Dev *et al.* 2010; Wang, Y *et al.* 2013). Utilising this method, chitosan has been used to coat onto the surface of the PLGA microparticle through physical adsorption (Wang *et al.* 2013). In this regard, coating is achieved by electrostatic attractive forces between the polycationic chitosan and the more negatively charge PLGA particle (Guo & Gemeinhart 2008). In the present study, by adding dissolved chitosan into the PVA surfactant prior to the formation of the double emulsion we envisage that the chitosan would form a coating on the surface and porous structure of the PLGA microparticles during the solvent evaporation phase.

## **4.2 Materials and Equipment**

Poly (lactic-co-glycolic acid) (PLGA) was obtained from Lakeshore Biomaterials, Poly (vinyl alcohol), 87-89% hydrolyzed, and Phosphate buffer saline (PBS) tablets (0.01M phosphate buffer, 0.0027M potassium chloride and 0.137M sodium chloride, pH7.4 at 25°C) was obtained from Sigma-Aldrich. Dichloromethane (DCM) AR grade was obtained from Fischer Scientific UK. Sodium hydroxide pellets was obtained from Sigma- Aldrich as well. Pure acetic acid purchased from Thermo Fisher Scientific (Bridgewater, NJ, USA).

Equipment used include Perkin Elmer FTIR spectrometer (Spectrum RX1, PerkinElmer Ltd, United Kingdom), Field Emission scanning electron microscopy (FESEM) equipped with an Energy dispersive x –ray detector (EDX) (Model Quanta 400F, FEI Company, USA), high speed homogeniser (IKAT-18, Cole-Palmer, Illinois, USA), Beckman Benchtop Centrifuge (Allegra X-22R, Beckman Coulter, Inc., Indianapolis, USA).

## **4.3 Methods**

### **4.3.1 General protocols for formulation of porous and non-porous PLGA microparticles**

The protocol was based upon the double solvent evaporation method, with an additional step involving the addition of 4-FPBA conjugated chitosan into the formulation.

100 mg of PLGA was dissolved in 5 ml of dichloromethane (DCM) in 50 ml beaker producing 2% w/v of PLGA solution (oil phase). The beaker was placed on the orbital shaker set to 30 rpm for 10 minutes to ensure the PLGA is fully dissolved. For formulations with induced porosity, 250 µl of PBS solution ( $W_1$  phase) was added to the

PLGA/DCM solution and homogenised using high speed homogeniser at 9000 rpm for 2 minutes to create the primary emulsion ( $W_1/O$ ). However, for non-porous formulations, 100  $\mu$ l of distilled water was added into the PLGA/DCM solution in place of PBS. Time and speed of the homogeniser was identical to the porous formulations.

The dissolved conjugated chitosan (1% acetic acid) was poured into a 400 ml beaker containing 200 ml of 0.3% w/v PVA solution ( $W_2$ ). The solution was gently stirred using a magnetic stirrer at speed 300 rpm for 30 min to ensure homogeneity. Next, the primary emulsion ( $W_1/O$ ) was added to the PVA-chitosan solution to form the secondary emulsion ( $W_1/O/W_2$ ) and homogenised at 6000 rpm for 2 minutes. The secondary emulsion was then stirred at 300 rpm under a fume cupboard for 4 hours to allow for solvent evaporation and particle hardening.

The solution was then poured into separate 50 ml centrifuge tubes and was centrifuged at 4500 rpm for 15 minutes. The non-porous formulations were then collected and washed with distilled and subjected to centrifugation in a similar manner. This washing cycle was repeated thrice to ensure residual solvent was eliminated from the particles. For the porous formulations, the particles were collected and stored for further treatment to enhance pore formation before undergoing the same washing cycle. Both formulations were then air dried by storing in a room temperature environment overnight. The formulations were stored at 4  $^{\circ}$ C dry air refrigerator for a maximum period of one week prior to characterisation. As the physical integrity of PLGA microparticles is affected by the storage temperature, duration of storage and size of the particles, the short storage time for the formulations prior to analysis was done to avoid significant aggregation that may influence characterisation of these samples (De & Robinson 2004). Both

formulations were done for each experimental run until the optimum protocols were established for characterisation analysis.

#### 4.3.2 Protocols to enhance porosity of particles

In the porous formulations, the collected particles were exposed to ethanolic –NaOH to enhance surface porosity. The ethanolic-NaOH was prepared by mixing 1.0M NaOH and 96% ethanol at a ratio of 30:70. 10 ml aliquot of ethanolic-NaOH was then added rapidly to a 50 ml centrifuge tube containing the sample whilst on a vortex mixer and was vortexed at 1400 rpm for 7 minutes. The sample was then centrifuged and the excess ethanolic-NaOH was discarded before proceeding to a similar washing cycle as the non-porous formulation. Different concentrations of NaOH ranging from 0.5M to 0.8M were evaluated in order to optimise the best condition for imparting porosity on the sample.

#### 4.3.3 Characterisation of PLGA microparticles by FESEM analysis

FESEM imaging was performed to identify the surface characteristics and size of the sample. A small amount of the dried sample was placed onto an FESEM imaging stub. The sample was then viewed under field-emission FESEM at 5.0 kV.

#### 4.3.4 Porosity Calculations

The porosity of the microparticles was calculated using equation 2,

$$Porosity \% = \left(1 - \frac{\rho_{apparent}}{\rho_{PLGA}}\right) \times 100 \dots \dots \dots (2)$$

The theoretical density of PLGA polymer ( $\rho_{PLGA}$ ) was taken from literature as 1.3 g/cm<sup>3</sup> (Polysciences 2016). The apparent density ( $\rho_{apparent}$ ) of the PLGA microparticles was calculated based upon the displacement method. Briefly, 5 ml of distilled water at room temperature was poured into a 10 ml graded measuring cylinder and the initial volume was recorded. While tilting the measuring cylinder, a recorded amount of PLGA microsphere sample was placed into the cylinder. The final water level was then recorded and the amount of water displaced by the sample represents the apparent volume of the sample. As distilled water was used at room temperature, 1 ml of volume displaced represent 1 cm<sup>3</sup> of the volume of sample. The apparent density can then be calculated from equation 3. All measurements were done in triplicates. A simple two-tailed t-test was performed with 95% confidence interval to check for significant differences between experimental results where necessary.

$$\rho_{apparent} = \frac{Mass}{Volume} \dots\dots\dots (3)$$

#### 4.3.5 Fourier transform infra-red analysis (FTIR)

FTIR analysis was needed to ascertain whether the conjugated chitosan was successfully coated onto the PLGA microparticle and to complement data from the DCS analyses. A small amount of the lyophilised sample was crushed gently with approximately 250 mg of KBr powder until homogeneous powder is obtained. The powder was then compressed under 6 tonnes of pressure (5000 psi) using a pneumatic table press to form a disc. The spectra were collected at the range of 4000- 400 cm<sup>-1</sup> with measurements done in triplicates for each sample.

## 4.4 Results and Discussion

### 4.4.1 Formulation of non-porous PLGA microparticles

Utilising the double emulsion solvent evaporation method, the non-porous PLGA microparticles were successfully formulated. Figure 13 shows the FESEM images of the non-porous formulation. The image was taken at 5.0 kV at 2500 x and 500 x magnification respectively.

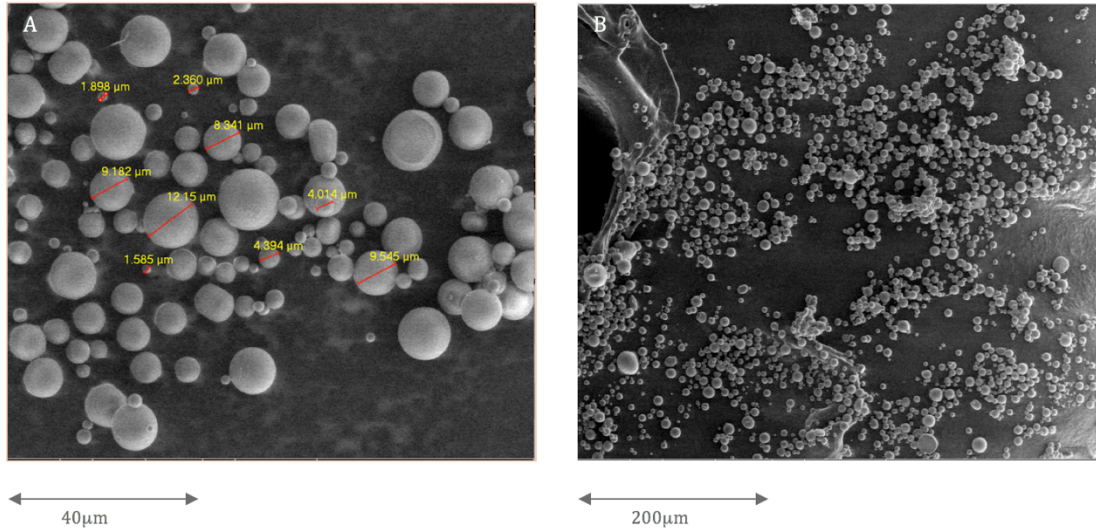


Figure 13: FESEM images of non-porous PLGA microparticles with A representing the FESEM image taken at 2500 X magnification and B at 500 X magnification.

From the FESEM image A in Figure 13, it can be seen that the non-porous formulation produced sub-micron PLGA particles that were non-porous as well, spherical in shape with relatively uniform size ranging from 1.0  $\mu\text{m}$  to 10  $\mu\text{m}$ . As the particles are sub-micron, particle size analyser specifically the Zetasizer Nano instrument was not suitable for calculating the mean particle size. However, it can be seen from the representative sample in figure 13 that the relative uniform size of the particles obtained demonstrate the

viability of the protocols used to formulate consistent non-porous PLGA microparticles and is adequate to fulfil the objectives of this study.

The stirring rate of the secondary emulsion plays a significant role in the particle size of the formulation as reported in a previous study on optimisation techniques for the formulation of PLGA microspheres (Birnbaum *et al.* 2000). The stirring rate used in the present study was set to 6000 rpm which was much higher than those reported in several microsphere formulation investigations and we believe this is the cause of the submicron sized particle production. Thus, nano-size PLGA particles can be achieved through the double emulsion method by gradually increasing the stirring rate of the secondary emulsion or by increasing the concentration of PVA surfactant. However, as the objective of the present study was to investigate the effects of porosity on the glucose sensitivity and insulin release from PLGA microparticles, the range of particle sizes obtained in this formulation were nonetheless adequate to carry out the objectives of this study.

Furthermore, the non-porous formulation showed very little aggregation as seen in the FESEM image B of Figure 13. This is due to the use of partially hydrolysed PVA (87%-89%) as opposed to fully hydrolysed PVA in the secondary aqueous phase. The degree of hydrolysis of the PVA plays a significant role in the aggregation of PLGA microparticles. As the degree of hydrolysis increases, the hydrophilicity of the PVA decreases which increases the hydrogen bonds between intra- and inter PVA molecules rather than with water molecule. The formation of these hydrogen bonds hinders the hydrophobic portions of the PVA to be absorbed to the surface of the PLGA particle which would result in unstable dispersion and agglomeration (Murakami *et al.* 1997). Murakami *et. al* (1997) found that by utilising PVA with high degree of hydrolysis (up to 98.5%) produced aggregated nanoparticles, leading to a decrease in the yield observed (Murakami *et al.*

1997). This was attributed primarily due to the increase in PVA-PVA hydrogen bonds leading to unstable nanoparticles. By using partially hydrolysed PVA, the PVA molecule was unhindered and can successfully be absorbed to the surface of the PLGA particle. In addition, the large amount of PVA solution used to emulsify the primary emulsion provides a large continuous phase for the precipitation of stable sub-micron particles. Both factors decreased the chances of aggregation and produced the stable PLGA microparticles seen in the figure.

#### **4.4.2 Optimisation of porous PLGA microparticle**

The protocol outlined in section 4.3.1 was used to formulate the porous PLGA microparticles. After centrifugation, the particles were exposed to ethanolic-NaOH to enhance the porosity within the particles as described by Qutachi *et al.* (2014) on their injectable PLGA microspheres (Qutachi *et al.* 2014). Their study describes the suitability of ethanolic –NaOH in producing uniform pores in PLGA microparticles since ethanol is a water- miscible solvent capable of partially dissolving PLGA while NaOH improves the polyester wettability by promoting the carboxylic acid exposure on the polymer surface making it more hydrophilic (Qutachi *et al.* 2014). This in effect causes the opening of the pores present on the surface of the particle resulting in a tangible increase in the overall porosity of the particle.

Figure 14 shows the FESEM images of the porous formulation after treatment with ethanolic –NaOH mixture at 1.0M NaOH. The images were taken at 5.0 kV at 2500 X and 500 X magnification.

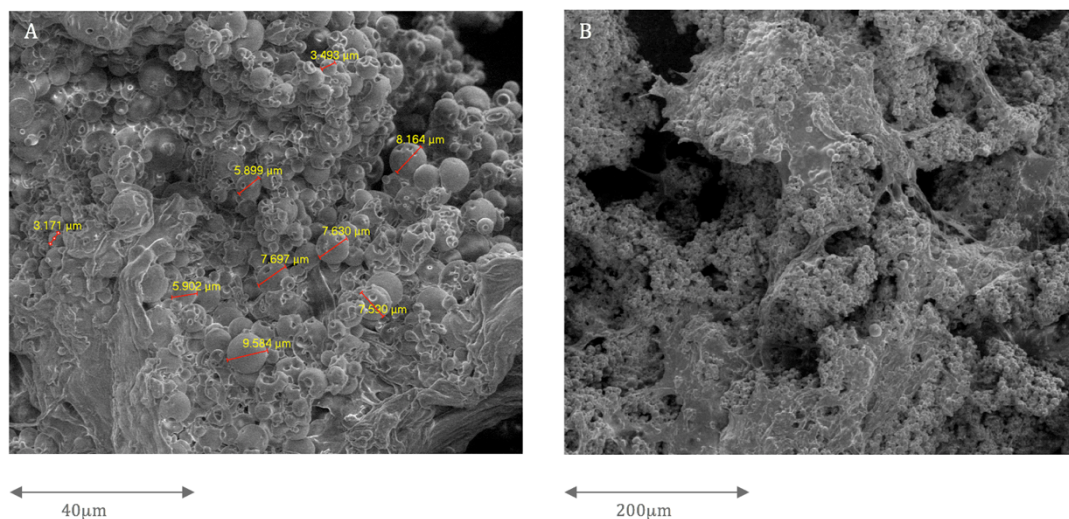


*Figure 14: FESEM images of porous PLGA microparticles with A representing the FESEM image taken at 2500 X magnification and B at 500 X magnification*

The FESEM image (A) in Figure 14 shows that upon addition of the ethanolic- NaOH, most of the PLGA microparticles were ruptured and failed to retain its spherical shape. Fragments of the PLGA particle were seen to be clumped to together forming large aggregate sections. Agglomeration was so severe throughout the sample shown in FESEM image B that discrete PLGA microparticles were hard to discern. While it was observed that in some of the particles there was evidence of pore formation, the particles were unstable and deemed unsuitable for drug loading applications. Therefore, this high strength of NaOH may not be suitable for imparting the required level of porosity without harming the integrity of the microparticles.

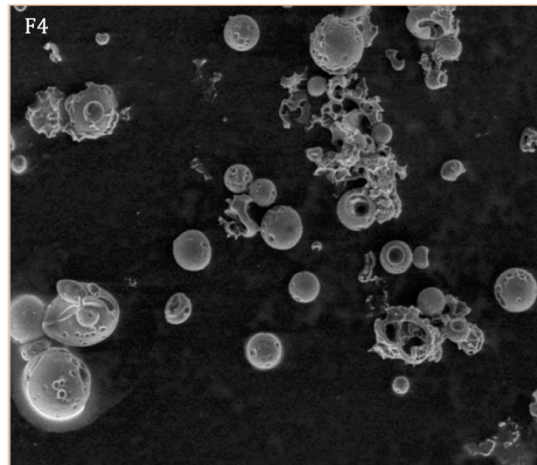
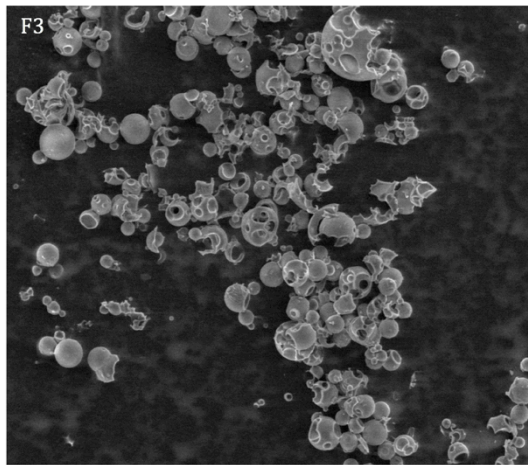
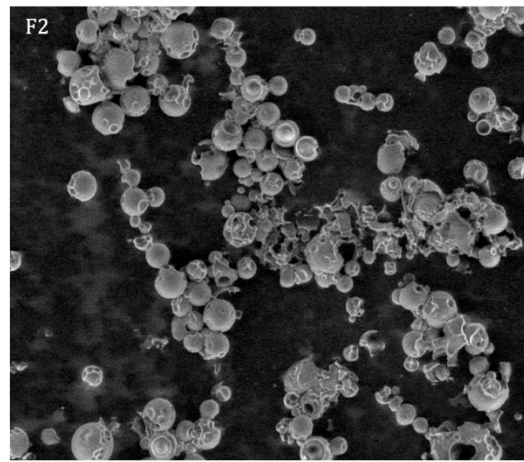
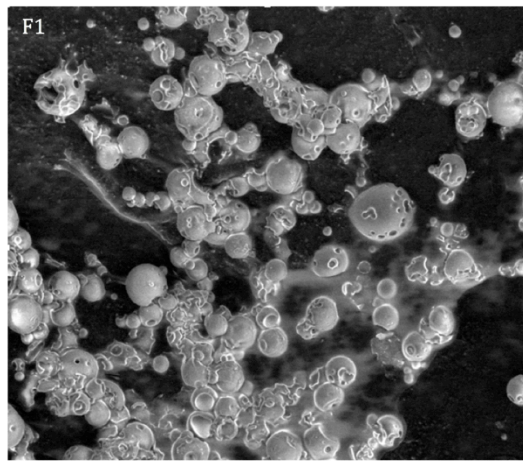
Further optimizations were to be carried out in order to strike the right balance for pore formation. The formulations studied are shown in Table 3 in which the concentration of sodium hydroxide was gradually decreased from 1.0M to 0.5M. Other factors such as the ratio of PLGA to chitosan as well as the speed and duration of the vortex mixer were kept constant.

Table 3: Optimisation of formulation for porosity of PLGA microparticles

<b>Formulation</b>	<b>PLGA (mg)</b>	<b>Chitosan (mg)</b>	<b>Conc. NaOH in Ethanolic-NaOH mixture</b>
<b>F1</b>	100	35	0.80 M
<b>F2</b>	100	35	0.70 M
<b>F3</b>	100	35	0.60 M
<b>F4</b>	100	35	0.54 M
<b>F5</b>	100	35	0.52 M
<b>F6</b>	100	35	0.51 M
<b>F7</b>	100	35	0.50 M

A report by Guo & Gemeinhart (2008) showed that as more chitosan was added into the PLGA nanoparticles, the size grew larger suggesting that the chitosan continually coats the surface of the particles in multiple layers (Guo & Gemeinhart 2008). Thus, by controlling the ratio of PLGA to chitosan in each formulation, the amount of chitosan incorporated can be regulated for each formulation. In order to accurately investigate the effects of the concentration of sodium hydroxide on the porosity observed, the amount of ethanolic- NaOH as well as exposure time were kept constant at the values set in the protocols described in 4.3.2.

The FESEM images of formulations F1 –F4 are shown in the Figure 15 and those for F5-F7 in Figure 16. The images were taken at 5.0 kV at 2500X magnification.



*Figure 15: The FESEM images of porous formulations F1 to F4 at 2500X magnification*

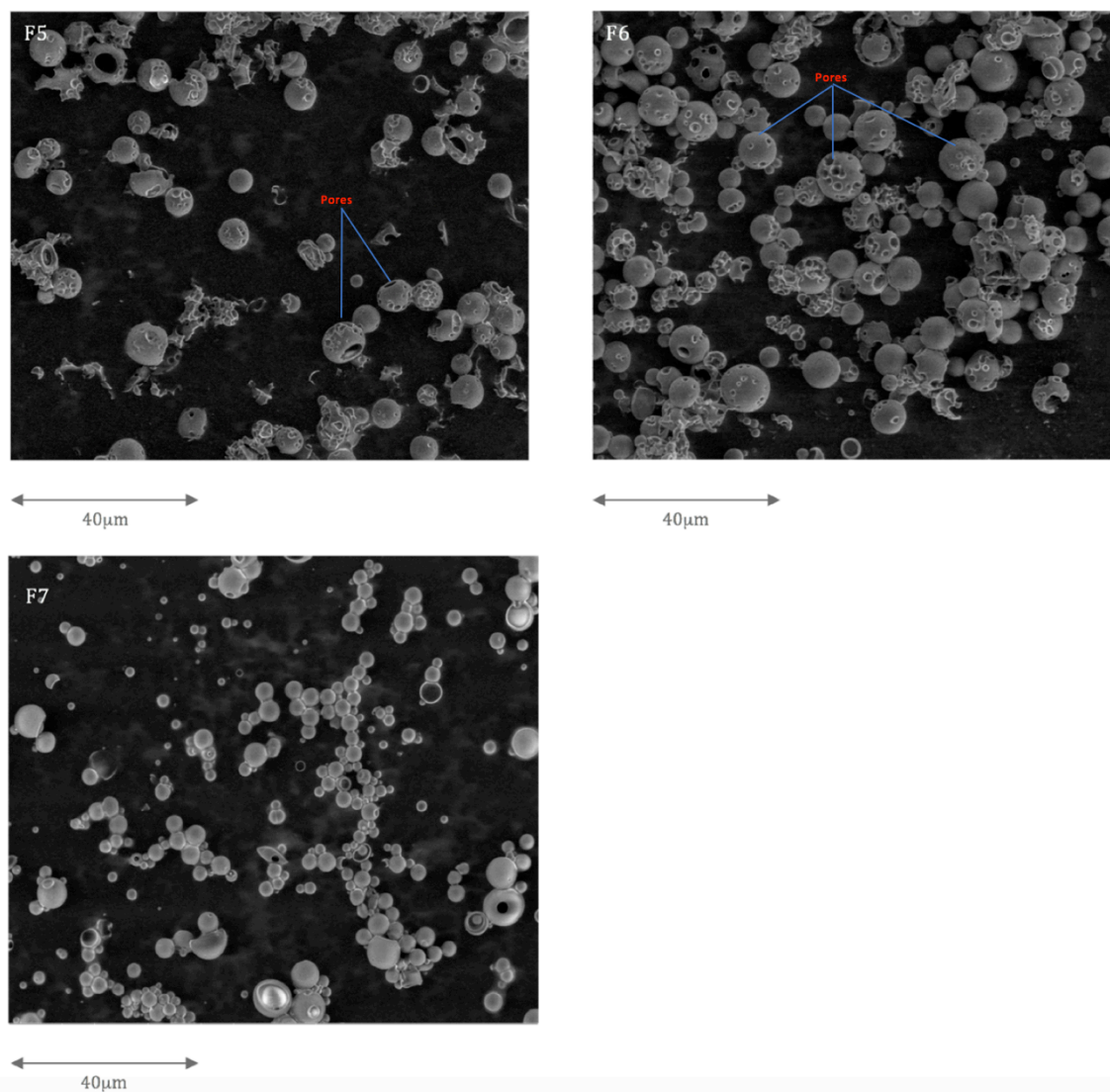


*Figure 16: The SEM images for porous formulations F5 to F7 at 2500X magnification*

From both figures, we observed a gradual change in the microstructure of the PLGA microparticles as the NaOH concentration in the ethanolic –NaOH mixture was decreased. At NaOH concentration of 0.80M to 0.54M (F1 to F4, Figure 15), exposure to ethanolic-NaOH resulted in the formulation having a similar but less severe fragmentation and agglomeration than those noted in the 1.0M NaOH formulation. However, as the concentration of NaOH was decreased below 0.54M, less fragmentation

of the PLGA particle was observed and the sub- micron particles formed were relatively stable. Concurrently, we can claim that the pores appear to decrease with decreased NaOH concentration. At NaOH concentration of 0.52M and 0.51M (formulations F5 and F6 shown in Figure 16), the PLGA microparticles retained their spherical shape with less agglomeration. Pores on the surface of the microparticles were also visible on the FESEM images in these formulations. Finally, at 0.50M NaOH, the formulation (F7) showed no porosity on the surface and the microparticles formed were discrete and stable which suggest that exposure of the microparticles to this concentration of NaOH in the the ethanolic- NaOH was inadequate to induce porosity on the surface of the particle without destroying the integrity of the particles. From this optimisation study, F6 presented the most desirable characteristics in terms of the nature of the pores discreteness fragmentation. Hence, F6 was used for subsequent investigations.

#### **4.4.3 Porosity Calculations**

Porosity calculation was done in order to quantify the degree of porosity within the microparticles in the porous and non-porous PLGA microparticles. In order to calculate porosity, the apparent density of the sample must be determined beforehand. The apparent density is defined as the mass per unit volume of the material, including the voids which are inherent in the material (Webb 2001). The apparent density was calculated based upon the displacement method.

Table 4 compares the porosity values with standard error in both porous and non-porous PLGA microparticle samples. All measurements were done in triplicates.

Table 4: Porosity values for non-porous and porous PLGA microparticles formulations

Sample	F1 (Non-porous PLGA MP)	F2 (Porous PLGA MP)
Mass Recorded (mg)	250	250
Apparent Volume (cm <sup>3</sup> )	0.20 ± 0.10	0.57 ± 0.03
Apparent Density (g/ cm <sup>3</sup> )	1.25±0.01	0.44 ± 0.02
Theoretical Density (g/ cm <sup>3</sup> )	1.30	1.30
Porosity %	3.88 ± 0.02	64.07 ± 1.74

An independent two sample t-test was conducted to compare the apparent density and porosity between the two formulations. With reference to Table 4, it can be seen that the apparent density of the porous PLGA microparticle formulation (M= 0.44 g/cm<sup>3</sup>, SD = 0.03 g/cm<sup>3</sup>) is lower than that of the non-porous sample (M= 1.25 g/cm<sup>3</sup>, SD = 0.02 g/cm<sup>3</sup>) owing to the increase in voids and pockets associated with porous microparticle as observed in the SEM images in Figure 16; t(3)= 3.18, p < 0.05. A decrease in apparent density in the PLGA microparticle sample correlates to higher porosity value as seen in the table. Overall, the porous PLGA microparticle showed a high porosity value (M= 64.07%, SD = 3.01%) as compared to the non-porous sample (M= 3.88%, SD= 0.03%); t(3)= 3.58, p < 0.05. This represents the maximum achievable porosity without compromising the structural integrity of the PLGA microparticles for the current protocols used in this study. The reported porosity is in line with other studies regarding injectable porous PLGA microspheres with porosity ranging from 66 to 74% showing measurable characteristic differences including drug release kinetics as compared to non-

porous variants (Qutachi *et al.* 2014). Thus, incorporating a porogen during the double solvent evaporation process as well as the additional exposure of the samples to ethanolic – NaOH provided a reproducible pathway to formulate porous PLGA microparticles.

#### 4.4.4 FTIR analyses on chitosan incorporated PLGA microparticles

One of the objectives of the present study was to produce PLGA microparticles coated with 4-FPBA conjugated chitosan in order to impart the glucose specificity on the insulin loaded PLGA microparticle. With the successful formulation of the non-porous and porous PLGA microparticles, an investigation was conducted to ascertain whether the 4-FPBA–conjugated chitosan was successfully incorporated into the PLGA microparticles. Comparisons between uncoated PLGA microparticle (Pure PLGA MP) and chitosan-coated formulations (PLGA MP F1 and PLGA MP F2) were required to accurately perform this investigation. The formulations were based on the protocol for the non-porous microparticles detailed in section 4.3.1. 4-FPBA conjugated chitosan with a high degree of substitution (aldehyde equivalent of 16) was used to coat the non-porous PLGA microparticle for ease of analysis. Table 5 shows the formulations used for FTIR analysis.

*Table 5: Formulations for chitosan coated PLGA microparticles studies*

<b>Formulation</b>	<b>PLGA (mg)</b>	<b>Conjugated Chitosan (mg)</b>	<b>Ratio PLGA: Chitosan</b>
Pure PLGA MP	100	0	1: 0
PLGA MP F1	100	35	1: 0.35
PLGA MP F2	100	70	1: 0.70

Figure 17 shows the FTIR spectra obtained from the PLGA microparticles formulated for this investigation. The spectra were collected at a range of 4000- 400  $\text{cm}^{-1}$ . The formulations were then compared to the FTIR spectra of pure chitosan.

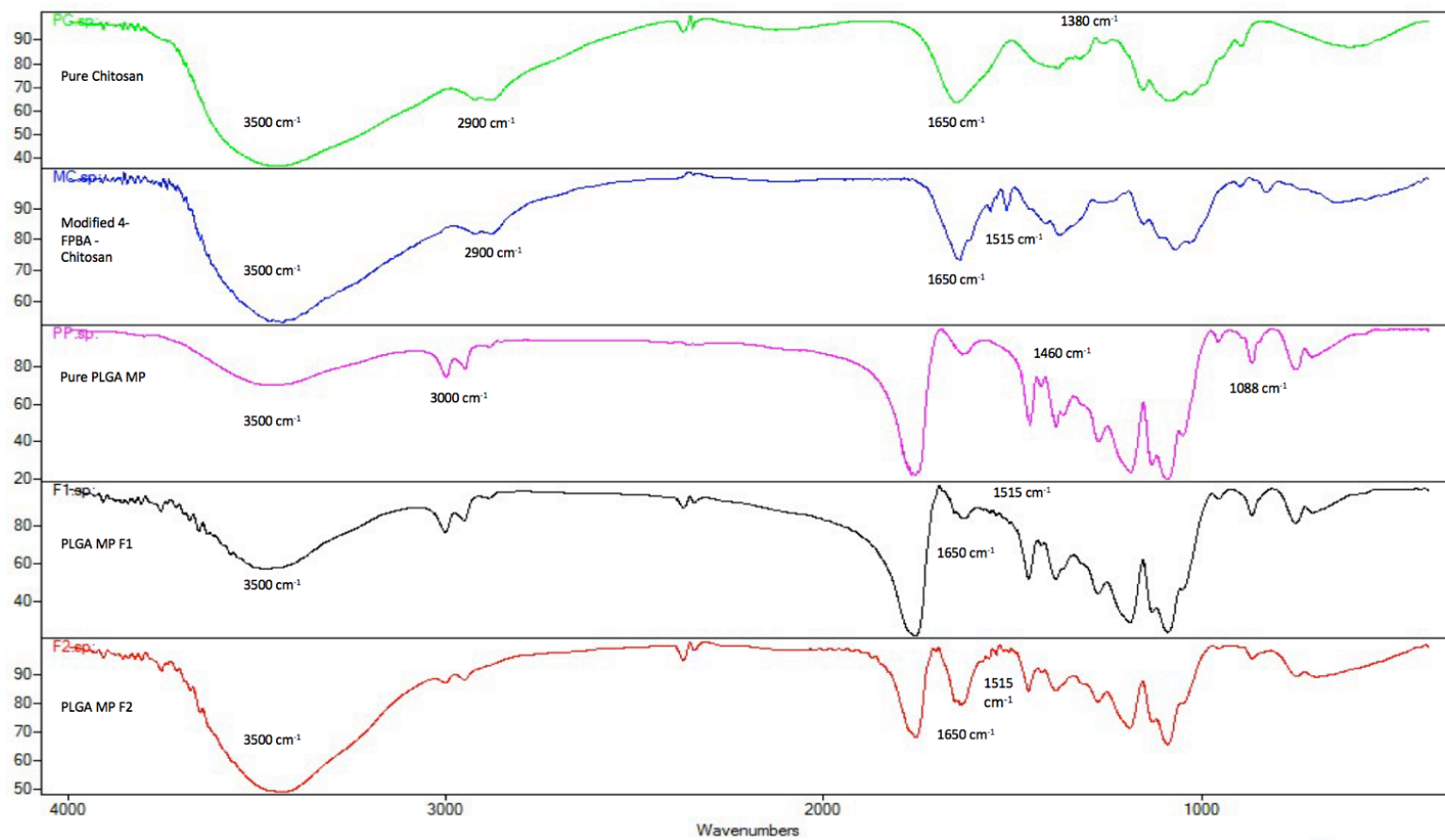


Figure 17: FTIR spectra of chitosan coated formulations with respect to uncoated PLGA microparticles (MP), pure unmodified chitosan and 4-FPBA-chitosan conjugates

With reference to Figure 17, pure chitosan is shown to have an intense peak at  $1650\text{ cm}^{-1}$  confirming the presence of the primary amine ( $-\text{NH}_2$ ) group in the chemical structure of chitosan (Ding *et al.* 2003). Note, the peak at  $1650\text{ cm}^{-1}$  was deemphasized after N-reductive alkylation reaction in which 4-FPBA was conjugated to chitosan as shown in the figure. Furthermore, C-H bond stretching was characterised as the peak in  $2900\text{ cm}^{-1}$  while C-H bend peak is shown in the range  $1360 -1440\text{ cm}^{-1}$ . Finally, N-H bond stretching was shown as a wide peak at  $3500\text{ cm}^{-1}$ .

In the uncoated (pure) PLGA microparticles FTIR spectra, the peak observed at  $1088\text{ cm}^{-1}$  is due to the C-O-C stretching while C-H stretching of the methyl group is characterised by the peak at  $1460\text{ cm}^{-1}$  (Wang *et al.* 2013). Other characteristic peaks of PLGA are between  $2850\text{ cm}^{-1}$  and  $3000\text{ cm}^{-1}$  are due to CH, CH<sub>2</sub> and CH<sub>3</sub> stretching vibration. Lastly, the peak at  $3500\text{ cm}^{-1}$  is due to OH stretching which overlapped the N-H bond stretching peak in pure chitosan sample.

It can be seen that the chitosan peak associated with N-H stretching was also present in the FTIR spectra of the chitosan coated PLGA microparticle formulations. As the peaks in the uncoated PLGA microparticles and pure chitosan overlaps at  $3500\text{ cm}^{-1}$ , the inclusion of chitosan in the formulation manifested an increase in the intensity of this peak as seen in F1. In addition, by doubling the ratio of PLGA: chitosan as in in F2 with respect to F1, the intensity of this peak was increased further. This result suggests that as the ratio of PLGA: chitosan was increased in the formulation, more of the chitosan was adsorbed on the surface of the PLGA particle. This observation is supported by a similar data reported by Guo & Gemeinhart (2008) on the adsorption mechanism of chitosan unto the surface of PLGA particles whereby the researchers postulate that as the amount

of chitosan was increased in the PLGA nanoparticle formulations, multiple layers of chitosan was formed on the surface of the PLGA nanoparticle (Guo & Gemeinhart 2008). Further analyses showed that another chitosan peak at  $1650\text{ cm}^{-1}$  was present in the chitosan coated PLGA microparticle formulations suggesting that the free amine group ( $\text{-NH}_2$ ) expressed in the chitosan backbone was also present in the microparticle formulations. Similarly, it was observed that the sharpness of this peak increased when the ratio of PLGA: chitosan was doubled as in F2 with respect to F1. More importantly, it can be seen that peaks at  $1515 - 1560\text{ cm}^{-1}$  characterised previously in 4-FPBA conjugated chitosan were present in F1 which resolves into greater detail in F2. Thus, through this procedure, we can confirm that the 4-FPBA conjugated chitosan was successfully incorporated within the PLGA microparticles.

## 4.5 Summary

The double solvent evaporation method was used to formulate both non-porous and porous chitosan coated PLGA microparticle. Utilising this method, the non-porous formulation showed spherical microparticles of relatively uniform sizes in the range of 1.0 to 10.0  $\mu\text{m}$  with no agglomeration. However, optimisation was required in order to formulate porous microparticles with desirable porosity and pore characteristics. The use of concentrated NaOH (1 M) in ethanolic-NaOH mixture to enhance porosity resulted in the rupture of most of the nanoparticles. This fragmentation then resulted in significant agglomeration which makes characterization of the particles difficult. By decreasing the concentration of NaOH to 0.515M, exposure to ethanolic-NaOH mixture resulted in porous PLGA microparticles of similar sizes to that of the non-porous formulation. The porous particles formed were spherical, stable with numerous pores observed on the surface.

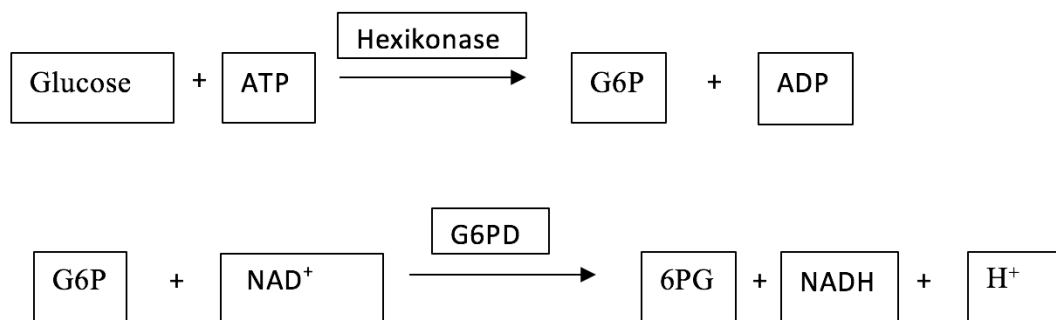
Through FTIR analyses, it was confirmed that modified chitosan was successfully incorporated in the PLGA microparticles with certain chitosan peaks present in the FTIR spectra of the PLGA microparticle formulations. Thus, the modified protocols that were added into the double solvent evaporation method to incorporate 4-FPBA conjugated chitosan is viable in producing coated PLGA microparticles.

## 5.0 GLUCOSE ABSORPTION BY PLGA MICROPARTICLES

### 5.1 Introduction

This chapter focusses on the glucose absorption propensities of both porous and non-porous PLGA microparticles. With the successful formulation of 4-FPBA modified chitosan- coated PLGA microparticles, we moved to the next objective of the study which is to evaluate the extent of the glucose absorption on the two types of microparticles (porous and non-porous). Matsumoto *et al.* (2002) managed to formulate chitosan gel that had been modified by phenylboronate for selective absorption of glucose (Matsumoto *et al.* 2002). To ascertain the adsorption capacity and selectivity of the modified chitosan gel compared to those of the commercial gel, the team used glucose and 1-methyl- $\alpha$ -D-glucoside as adsorbates. Phenylboronate anion is known to form complexes with cis-1,2 or 1,3 diols which are both present in glucose (Matsumoto *et al.* 2002). The study by Matsumoto *et al.* (2002) concluded that the phenylboronate chitosan gel provided a higher absorption of glucose compared to 1-methyl- $\alpha$ -D-glucoside. Thus, boronic acid and their derivatives was proven to be sensitive towards glucose based on the findings of Matsumoto *et al.* (2002) as well as numerous other studies regarding glucose sensitive boronic acid materials (Matsumoto *et al.* 2002; Jennifer N. Cambre & Sumerlin 2011). However, it was found that it is difficult to directly characterised glucose via UV- spectroscopy and indirect methods are required to accurately determine the absorbance of glucose in this study.

One method of indirectly measuring the absorbance of glucose involves the use of glucose hexokinase reagent (Galant *et al.* 2015). The reaction involves glucose being converted to glucose-6-phosphate and nicotinamide adenine dinucleotide (NAD<sup>+</sup>) in the presence of enzyme hexokinase (HK). Glucose-6-phosphate by-product is then oxidised to 6-phosphogluconate by glucose-6-phosphate dehydrogenase while nicotinamide adenine dinucleotide (NAD<sup>+</sup>) is reduced to NADH. NADH can then be detected by UV-spectroscopy at 340 nm. The overall reaction is shown in figure 18.



Where:

ATP/ADP = Adenosine triphosphate/ Adenosine diphosphate

G6P = Glucose-6-phosphate

NAD<sup>+</sup>/ NADH = Nicotinamide adenine dinucleotide

6PG = 6-phosphogluconate

Figure 18: Overall conversion of glucose to detectable NADH by reaction with hexokinase reagent

Another method of indirectly measuring glucose absorbance is by utilising curcumin to directly detect boronic acid derivatives. Curcumin has been used to detect boronic acid and their derivatives in previous studies due to ease of analysis with UV-spectroscopy (Lawrence *et al.* 2012; Siddiqui *et al.* 2017). Curcumin reacts readily with boronic acid to form a complex (rosocyanine) and can be easily detectable at a wavelength of 425 nm. Furthermore, the complex rosocyanine shown in Figure 19 forms a solution of bright red

in colour (Lawrence *et al.* 2012). The characteristic colour change from yellow (curcumin) to red on formation of the complex can also be used as a visual indicator for the presence of boronic acid derivatives.

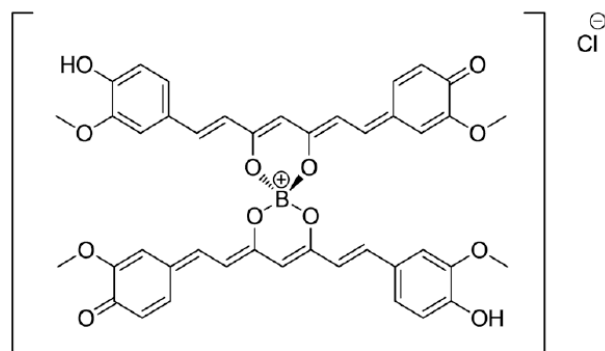


Figure 19: Chemical structure of rosocyanine complex

The two indirect methods discussed are viable methods to investigate the glucose absorption propensity of the microparticles. However, the more suitable method used in the present study was by curcumin reaction with 4-FPBA content in the chitosan coated PLGA microparticles in an HPLC analysis. This provided an efficient and easier analyses as well as providing visual feedback through the colour change brought upon by the rosocyanine complex. Figure 20 shows the overall reaction of the 4-FPBA-chitosan coated PLGA microparticle with curcumin. By determining the amount of 4-FPBA in both porous and non-porous formulations of PLGA microparticles, the difference in absorbance of curcumin between the two formulations would give an indirect indication of the sensitivity of the PLGA microparticles towards glucose.



*Figure 20: Overall reaction between 4-FPBA modified chitosan coated PLGA microparticles and curcumin*

## **Materials and Equipment**

HPLC grade acetonitrile and methanol obtained from Thermo Fischer Scientific (New Jersey, USA), pure acetic and curcumin purchased from Thermo Fisher Scientific (Bridgewater, NJ, USA). Poly (lactic-co-glycolic acid) (PLGA) was obtained from Lakeshore Biomaterials, low molecular weight chitosan was purchased from Sigma Aldrich (St.Louis,MO, USA); 4-formylphenylboronic acid (4-FPBA) and sodium borohydride was purchased from Thermo Fisher Scientific (Bridgewater, NJ, USA). Type one ultrapure Milli-Q<sup>®</sup> Water (18.2 ohms at 25<sup>0</sup>C) obtained from Merck Sdn. Bhd. (Selangor, Malaysia).

Equipment used include HPLC (Perkin Elmer, Shelton, Connecticut, USA), HPLC column with the specification of Agilent Zorbax 300SB-4.6 x 250 mm C18, with particle size of 5 µm and pore size of 300 Å (Agilent Technologies, California, USA), Beckman Coulter Microfuge 16 centrifuge (Beckman Coulter, Inc., Indianapolis, USA).

## **5.2 Method**

### **5.2.1 HPLC analysis for glucose adsorption**

The HPLC solvent system comprised of acetonitrile as solvent A, 0.01 % acetic acid as solvent B and methanol as solvent C in the ratio 53:42:5. The flowrate was set to 1.5 ml/min with isocratic elution. The detection wavelength was set to 425 nm with an injection volume of 10 $\mu$ l. Elution was through an Agilent Zorbax 300SB-4.6 x 250 mm C18, with particle size of 5  $\mu$ m and pore size of 300 Å.

The calibration curve was constructed from curcumin solution dissolved in methanol ranging from 0-50  $\mu$ g/ml. A calibration curve of average peak height against curcumin concentration was then constructed and the coefficient of determination ( $R^2$ ) and equation of the line were determined. Preparation of sample involved measuring 10 mg of each sample into a micro-centrifuge tube. The sample was then exposed to 1 ml of mili-Q water before addition of 500  $\mu$ l of 0.1 mg/ml of curcumin solution. To calculate the absorbance of free curcumin, the mixture was centrifuged at 14000 rpm for 2 minutes and 10  $\mu$ l of the supernatant was injected into the HPLC system. Samples were run in triplicates.

### **5.2.2 Yield analysis of the 4-FPBA conjugated chitosan PLGA microparticles**

The yield was calculated to observe any quantifiable differences in 4-FPBA content due to the porosity of the chitosan incorporated PLGA microparticles. The initial weight was based upon the total weight of PLGA and modified chitosan used in the formulation of PLGA microparticles.

Briefly, after formulation of both porous and non-porous PLGA microparticles as documented in section 4.3.1 and 4.3.2, the samples were freeze dried for up to 48 hours to ensure all moisture was eliminated. The recorded weight of the dry samples was then compared to the initial weight and yield. Yield analysis was done on three separate batches of formulations in order to get an average yield for the samples.

## 5.3 Results and Discussion

### 5.3.1 HPLC analysis of curcumin

The HPLC system was set to detect curcumin at a wavelength of 425 nm. Figure 21 shows the chromatogram of curcumin standard solution of 50  $\mu\text{g/ml}$  after a sample run of 5 minutes. It can be seen that there is one clearly resolved peak representing the curcumin peak at an elution time of approximately 2.3 minutes.

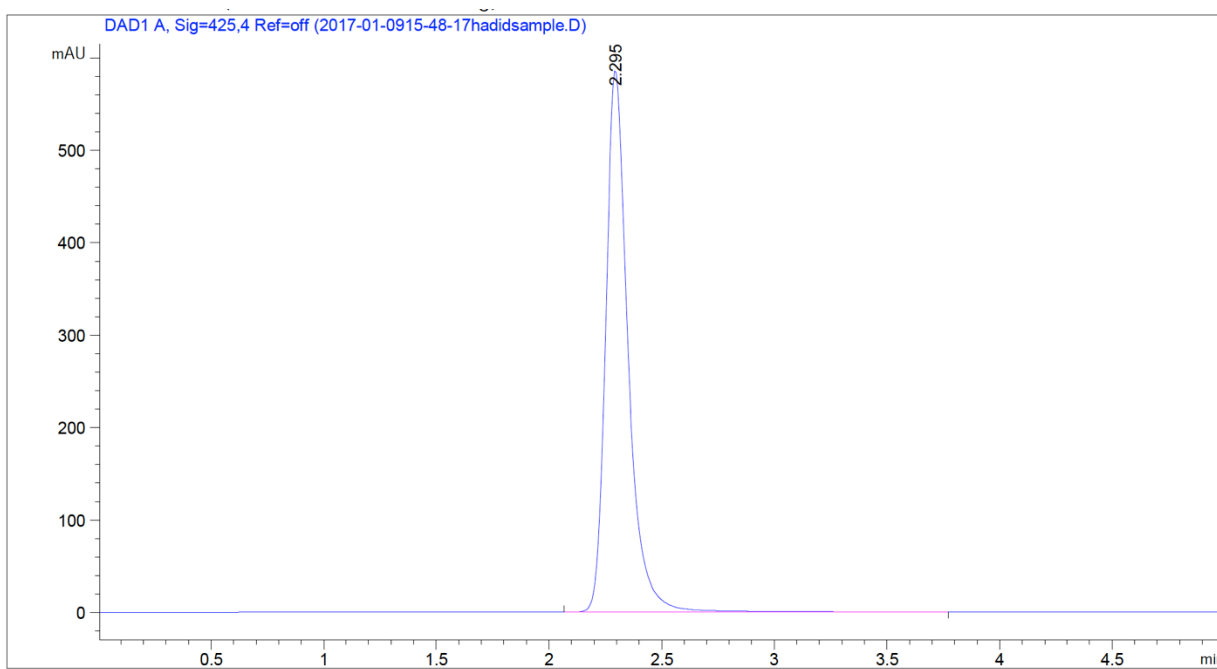


Figure 21: Chromatogram of curcumin standard solution 50  $\mu\text{g/ml}$

The calibration curve was constructed from curcumin standard solution range of 50 to 0  $\mu\text{g/ml}$ . Figure 22 shows the calibration curve of curcumin standard solution. The calibration curve was constructed by plotting the peak height with curcumin concentration. It can be seen from the figure that the peak height was proportional to the

curcumin concentration which gave the standard curve a good linearity reflected by the coefficient of determination ( $R^2$ ) value of 0.999.

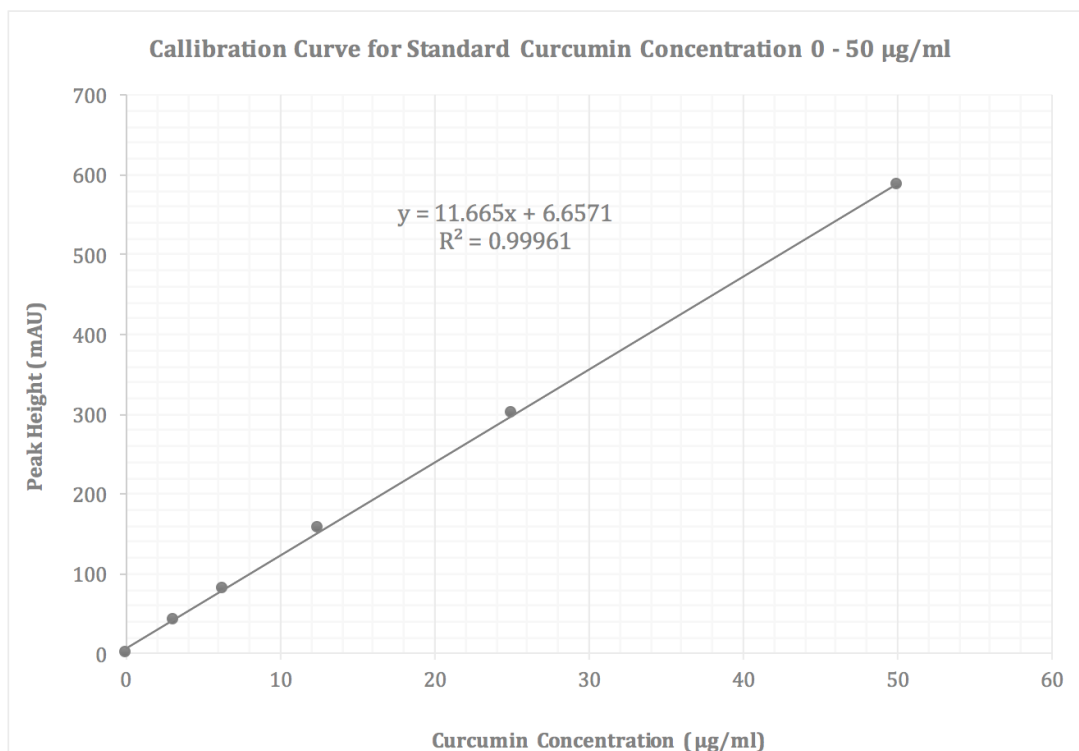


Figure 22: Calibration curve for curcumin standard solution 0 – 50 µg/ml

Limit of detection (LOD) and limit of quantitation (LOQ) was also determined by utilising the calibration curve in figure 22. In general, LOD represents the lowest concentration of an analyte in a sample that can be detected, but not necessarily quantified under the stated conditions of the study (Shrivastava & Gupta 2011). On the other hand, the LOQ is defined as the lowest concentration of an analyte in a sample that can be determined with acceptable precision and accuracy under the stated conditions of the test (Shrivastava & Gupta 2011). As the HPLC system was calibrated to eliminate baseline noise as observed in figure 21, the linear regression method was used to determine both LOD and LOQ as it is the most applicable method that does not involve

background noise and is most effective for range of low values close to zero for the calibration curve (Shrivastava & Gupta 2011). For a linear calibration curve, it is assumed that the instrument response  $y$  is linearly related to the standard concentration  $x$  for a limited range of concentration. This is the underlying assumption in constructing the calibration curve in figure 22. This linear regression model can be used to compute both LOD and LOQ respectively using the following equations (Shrivastava & Gupta 2011).

$$LOD = \frac{3S_a}{b} \dots\dots\dots(4)$$

$$LOQ = \frac{10S_a}{b} \dots\dots\dots(5)$$

where

$S_a$  is the standard deviation of the  $y$ -residuals of the regression line.

$b$  is the slope of the calibration curve

By utilising the LINEST function in Microsoft Excel software<sup>®</sup> to calculate the standard deviation of the  $y$ -residuals of the regression line (2.70), the calculated values of LOD and LOQ utilising equations 4 and 5 are 0.69  $\mu\text{g/ml}$  and 2.32  $\mu\text{g/ml}$  respectively. As the lowest concentration used to construct the calibration curve (3.12  $\mu\text{g/ml}$ ) is higher than both LOD and LOQ concentrations, the HPLC system used in this study is deemed fit for purpose and subsequent curcumin concentrations can be reliably and accurately determined using the aforementioned calibration curve.

As discussed previously, 4-FPBA reacts with curcumin forming a rosocyanine complex mixture. Initially, the curcumin concentration that was added into the samples was set to 0.1 mg/ml. By measuring the free curcumin that is unreacted in the final mixture, comparisons can be made between the amount of 4-FPBA in the chitosan coated PLGA microparticle in the porous and non-porous samples. The concentration of free curcumin was determined from the standard curve obtained in Figure 22, which was then used to calculate the percentage of curcumin consumed by the samples utilising equation 6.

$$\begin{aligned}
 & \textit{Curcumin consumed \%} \\
 & = \frac{(\textit{Final curcumin concentration} - \textit{Initial curcumin concentration})}{\textit{Initial curcumin concentration}} \times 100
 \end{aligned}
 \tag{6}$$

Figure 23 shows the percentage of curcumin consumed by the non-porous PLGA microparticle sample (F1) and the porous PLGA microparticle sample (F2).

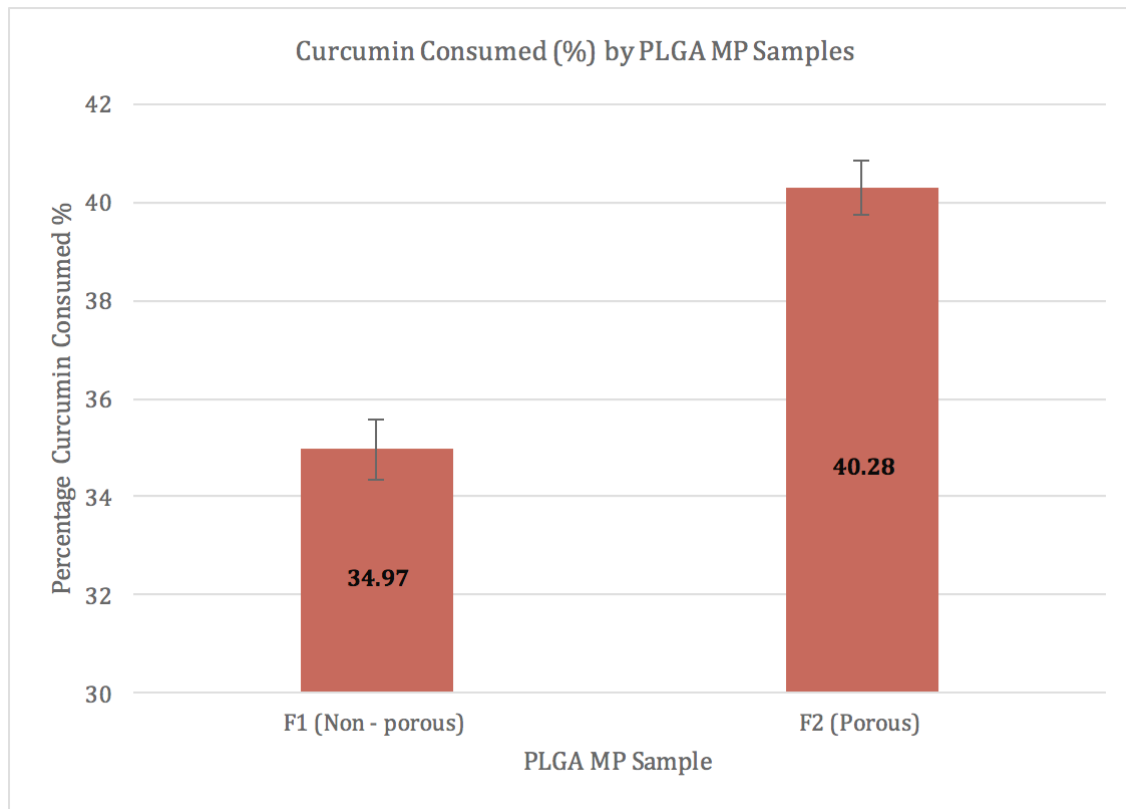
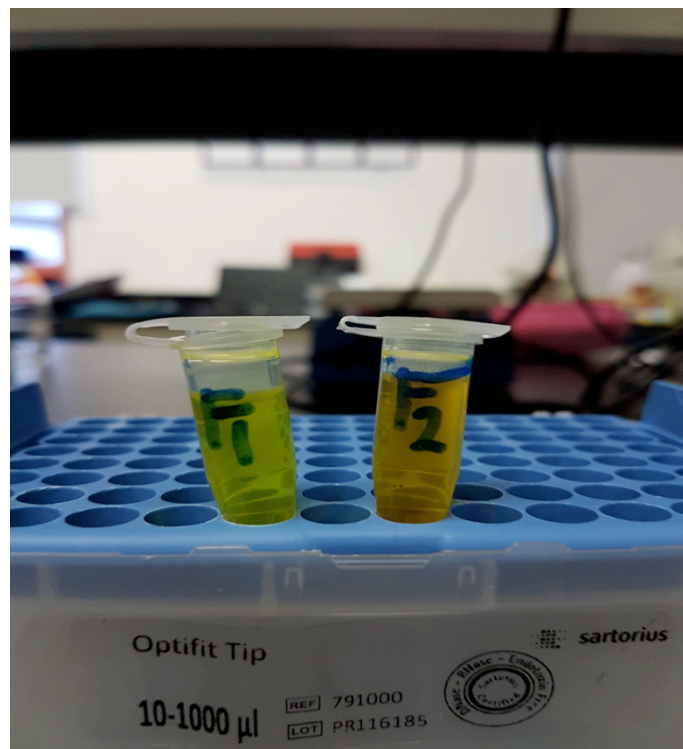


Figure 23: Curcumin consumption (%) of non-porous and porous PLGA microparticles, n=3

It can be seen that the percentage of curcumin consumed from the porous chitosan coated PLGA microparticles (F2) was notably higher than that of the non-porous sample (F1). This result showed definitively that the amount of 4-FPBA content was inherently higher in the porous microparticle sample which caused the increased in curcumin consumed in the reaction.

It was observed that an approximately 5% increase in the percentage of curcumin consumed for F2 was due to the highly porous structure of the PLGA microparticle. We may conclude that the porous structure afforded by the PLGA microparticle leads to an increase in surface area available for coating (Ilyas *et al.* 2013). Thus, more of the modified chitosan with 4-FPBA was able to coat upon the surface of the PLGA

microparticle and was more readily available to react with curcumin. In comparison, the non-porous PLGA microparticle sample provided less surface area for chitosan to be coated onto leading to a decrease in the amount of 4-FPBA available for reaction with curcumin. As 4-FPBA is documented to be sensitive to glucose, it can be said that the porous chitosan coated PLGA microparticle sample (F2) is likely to provide a better overall sensitivity characteristic towards glucose as compared to the non-porous sample. In addition to HPLC measurement, the formation of rosocyanine leads to a change in colour of the mixture. The intensity of the colour change between the samples F1 and F2 gives a visual comparison of the concentration of 4-FPBA in each sample. Figure 24 shows the colour change for sample F1 and F2 after addition of curcumin, note the initial colour of curcumin was bright yellow in standard solution.



*Figure 24: Color change exhibited by non-porous PLGA microparticle (F1) and porous PLGA microparticles (F2) upon reaction with curcumin*

It was observed that the colour change of sample F2 was more intense than F1 in Figure 24 with the mixture changing colour from initial bright yellow to orange. The colour change of F1 was less discernible suggesting significantly lesser amount of the rosocyanine complex formed in the mixture. This visual comparison corroborates the results obtained from the HPLC analysis whereby the amount of 4-FPBA available for reaction with curcumin to form the rosocyanine complex was notably higher in the porous PLGA microparticle owing to the increased in surface area available for chitosan coating.

### 5.3.2 Yield analyses

Yield analyses was performed in order to further quantify and compare the difference in 4-FPBA content available for curcumin detection in porous and non-porous PLGA microparticle samples. Yield was calculated based on the initial weight of materials added into the formulation. Both samples consist of 100 mg of PLGA and 35 mg of 4-FPBA modified chitosan as per the PLGA: chitosan ratio of 1: 0.35. The lyophilised samples were measured as the final dry weight of the microparticles and assumed to have negligible moisture content. The yield was then calculated based on equation 7 and all values are tabulated in Table 6.

$$Yield \% = \frac{(Final\ dry\ weight - Initial\ weight)}{Initial\ weight} \times 100 \dots \dots \dots (7)$$

Table 6: Yield of 4-FPBA in non-porous and porous PLGA microparticles formulations

Sample	F1 (Non-porous PLGA MP)	F2 (Porous PLGA MP)
<b>Initial weight (mg)</b>	135	135
<b>Dry weight (mg)</b>	65.0 ± 2.38	83.9 ± 2.29
<b>Yield %</b>	48.2 ± 1.76	62.1 ± 1.69

The yield for porous PLGA microparticle sample was observed to be higher (62.1%) than the non-porous PLGA microparticle sample (48.2%) as seen in Table 6. This results postulates that the highly porous structure in F2 resulted in an increased in surface area available for coating. Thus, the increase in available surface area afforded by the more porous network within the microparticles caused more of the modified chitosan to be retained in the formulation resulting in a higher yield percentage. In contrast, the limited surface area available for incorporation by the non-porous microparticles (F1) resulted in less of the modified chitosan to be incorporated in the final formulation showing a lower yield percentage. This result corroborates the findings in the curcumin analyses whereby the amount of curcumin consumed by the porous PLGA microparticles was higher than in the non-porous sample which gives an indication that the amount of detectable 4-FPBA was higher in the porous microparticle sample. The yield calculated here gives a more accurate quantification on the amount of 4-FPBA available present in the microparticles for curcumin detection. Thus, with both results, we can say that the highly porous structure of the PLGA microparticle was able to incorporate more of the modified

chitosan and consequently, a higher detectable 4-FPBA content as well as provide a larger effective surface area for curcumin – 4-FPBA interaction to facilitate the higher glucose absorption characteristic observed.

## 5.4 Summary

The glucose absorption of the PLGA microparticle samples was successfully ascertained through an indirect method of utilising curcumin to detect 4-FPBA content in the microparticle sample. By comparing the curcumin concentration before and after reaction with PLGA microparticles, the percentage of curcumin consumed by the boronic acid moieties within the microparticles was determined.

From the HPLC analyses, it was found that the porous PLGA microparticles consumed more curcumin compared to the non-porous sample. The increase in surface area afforded by the porous PLGA microparticle caused more of the modified chitosan to be coated onto and in the interstitial layers of the particles. This in turn, resulted in a higher amount of 4-FPBA readily available for reaction with curcumin in the porous microparticle sample. This theory is further supported by the drastic colour change in the porous microparticle mixture upon addition of curcumin whereby the bright yellow colour of curcumin changed to orange due to the formation of rosocyanine complex. The intense colour change observed showed that significant rosocyanine complex was formed in the reaction between curcumin and porous microparticle sample and confirms a higher concentration of 4-FPBA was readily available for the reaction.

A yield analysis was done to provide more insight into the glucose sensitivity of the two types of PLGA microparticle samples. The yield analysis quantifiably showed that a higher 4-FPBA content was obtained for the porous PLGA microparticle sample as compared to the non-porous sample. The yield analysis in this instance is related to the amount of 4-FPBA available for detection by curcumin. The porous microparticles, due to their porous microstructure, have a larger effective surface area for interaction with

curcumin and therefore should be more sensitive to glucose. On the other hand, the non-porous microparticles with a relatively smaller size dimension should also offer a large surface area. The next section of study would shed some light on the relative dominance of these two factors. 4-FPBA and other boronic acid derivatives have a documented history of being sensitive to glucose and thus being developed as glucose sensing devices in the field of medical science (Jennifer N Cambre & Sumerlin 2011; Guan & Zhang 2013). By measuring the 4-FPBA content in the PLGA microparticle through reaction with curcumin solution, the sensitivity of the microparticles towards glucose can be indirectly inferred. From HPLC and yield analyses, it was found that chitosan incorporated porous PLGA microparticles had a higher 4-FPBA content than the chitosan incorporated non-porous PLGA microparticle sample. We may affirm that the higher the 4-FPBA content in the porous PLGA microparticles would manifest a higher sensitivity towards glucose but as mentioned earlier, the non-porous samples are relatively smaller in size and it would be interesting to observe the relative responses of the two types of microparticles to glucose. This is expanded further in the insulin release studies discussed in the next chapter.

## 6.0 ENCAPSULATION AND RELEASE OF INSULIN FROM MODIFIED CHITOSAN COATED PLGA MICROPARTICLES

### 6.1 Introduction

This chapter details the extent of insulin encapsulation in chitosan coated porous and non-porous PLGA microparticles. Further studies were done to investigate the insulin release profiles from both types of microparticles in glucose media in order to assess the relationship between insulin release and the glucose absorption capacity of the microparticles as a function of porosity. This constitutes the final aim of the study.

The formulation of PLGA microparticles was achieved through the double solvent emulsion method ( $W_1/O/W_2$ ). The method was chosen due to the ease with which hydrophilic drugs such as insulin can be incorporated easily within the microparticles as well as the manifestation of sustained drug release rates studies (Hirenkumar & Siegel 2012). The double solvent evaporation method involves first producing the water in oil phase ( $W_1/O$ ) by dissolving PLGA in the chosen solvent. At this stage, the model drug is usually added into the first water-in-oil phase prior to homogenization. Once the emulsification of the second phase ( $W_1/O/W_2$ ) is achieved by the addition and homogenisation with the chosen surfactant, the drug should be encapsulated into the microparticle.

The encapsulation efficiency in the double solvent- emulsion method for formulating drug loaded PLGA microparticles is normally high with studies reporting efficiencies ranging from 60 % to close to 100% with variation observed from case to case (Yang *et*

*al.* 2009; Dev *et al.* 2010). Yang *et al.* (2009) utilised a similar method to formulate porous PLGA microparticles for pulmonary drug delivery with lysozyme and doxorubicin as the model drugs with a remarkably high encapsulation efficiency (approximately 100% for both model drugs) (Yang *et al.* 2009). In another study, chitosan coated PLGA nanoparticles utilised the hydrophilic drug Lamivudine for anti-HIV drug delivery applications reported a drug encapsulation efficiency of approximately 76% (Dev *et al.* 2010). Both studies showed the viability of drug encapsulation for PLGA particulates specifically formulated from the double solvent-emulsion method. However, a study by Wang *et al.* (2013) on the investigation of chitosan-modified PLGA nanoparticles with versatile surface for improved drug delivery found that increasing the amount of chitosan in the formulation contributed to a lower drug encapsulation (Wang *et al.* 2013). Thus, in this study, it is expected that the drug encapsulation efficiency for PLGA microparticle to be lower than expected as well since a significant amount of chitosan (chitosan: PLGA ratio of 0.35:1) was used in the formulation to coat the microparticle.

Various studies on the use of boronic acid and their derivatives to formulate glucose sensitive hydrogels reported that the hybrid gel showed considerable swelling termed 'glucose-dependent swelling behaviour' in the presence of glucose (Guan & Zhang 2013). This characteristic swelling can be detected by electrochemical means such as Faradaic impedance spectroscopy, chronopotentiometry and cyclic voltammetry which form the foundation for the development of glucose sensing devices (Guan & Zhang 2013).

While glucose sensing devices and hybrid devices show promising developments, the relatively newer field of utilising similar boronic acid moieties for formulating glucose responsive microparticles for insulin delivery shows potential as well. It is postulated in

this study that the same swelling behaviour exhibited by glucose sensitive hydrogels can be exploited to the insulin loaded PLGA microparticles so that swelling of the microparticles can trigger the release of insulin. Therefore, with the demonstrable glucose sensitivity, these microparticles should exhibit insulin in the presence of glucose. The introduction of porosity to the microparticles, means that there is a large surface area available for interaction between glucose and the boronic acid moieties available on the surface and interstitium of the microparticles. This in turn we hope would orchestrate a responsive release of insulin. Thus, in this last and crucial objective of this study we hope to compare the insulin release profiles of these glucose responsive porous and non-porous PLGA microparticles in glucose solution. In accomplishing this objective, conclusions can then be drawn on the effects of glucose sensitivity of the microparticles on the insulin release.

## 6.2 Materials and Equipment

Materials used for drug loading and release studies in addition to the materials required for PLGA microparticle formulation include HPLC grade acetonitrile and pure acetic acid obtained from Thermo Fischer Scientific (New Jersey, USA), Trifluoroacetic acid (TFA) acid 99% obtained from Sigma Aldrich (St.Louis,MO, USA), Insulin, recombinant human dry powder and Anhydrous D-(+)- Glucose was also obtained from Sigma Aldrich (St.Louis, MO, USA). Type one ultrapure Milli-Q<sup>®</sup> Water (18.2 ohms at 25<sup>0</sup>C) obtained from Merck Sdn. Bhd. (Selangor, Malaysia).

Equipment used include HPLC (Perkin Elmer, Shelton, Connecticut, USA), HPLC column with the specification of Agilent Zorbax 300SB-4.6 x 250 mm C18, with particle size of 5 µm and pore size of 300 Å (Agilent Technologies, California, USA), Beckman Coulter Microfuge 16 centrifuge (Beckman Coulter, Inc., Indianapolis, USA), Beckman Benchtop Centrifuge (Allegra X-22R, Beckman Coulter, Inc., Indianapolis, USA).

## **6.3 Methods**

### **6.3.1 Formulation of insulin loaded PLGA microparticles**

As insulin is only partially soluble in water, a more acidic solution was required to fully dissolve insulin powder. 5 mg of dry insulin powder was added into a 50 ml beaker containing 10 ml of 0.01 M acetic acid solution and was stirred thoroughly forming an insulin standard stock solution of 500 µg/ml. 1 ml of the insulin stock solution was then pipetted into a magnetically stirred chitosan solution which was then left stirring for 20 minutes to ensure the mixture was well homogenous. The mixture was then added into the poly (vinyl alcohol) (PVA) surfactant solution and all further steps in the formulation is as described in section 4.3.1. Both porous and non-porous insulin loaded PLGA microparticles were formulated for insulin release study.

### **6.3.2 HPLC analyses for insulin standard solution**

Insulin in the PLGA microparticle samples were detected using a Perkin Elmer quaternary HPLC system equipped with a UV detector. The mobile phase was 0.1% aqueous trifluoroacetic acid (TFA) (A) and 0.1% TFA in acetonitrile (B). TFA was added to the mobile phase at low concentration to ensure good peak shape was attainable in the chromatograph. It was reported that the use of TFA concentration of approximately 0.1% resulted in a good peak shape for most columns when used for the detection of insulin and other peptides (Carr 2016). While lowering the concentration of TFA further may improve the LC-MS detection sensitivity, it may result in poorly resolved peak shape especially for silica columns such as Agilent Zorbax due to the inherent purities in the silica surface (Carr 2016). A gradient elution of the mobile phase was used with mobile

phase A set to 75% of the total mobile phase and decreasing to 40% over 7 minutes at a flowrate of 1 ml/min. Insulin being protein would elute when the concentration of the organic solvent phase (B) increases to the precise concentration required for desorption (Carr 2016). In this case, isocratic elution is rarely useful for the separation of protein-based compounds like insulin because peaks obtained become broader and may result in loss in peak sharpness (Carr 2016). In addition, isocratic elution may cause large changes in the retention time if there is a small change in the organic solvent concentration of the mobile phase (Carr 2016). The injection volume was set at 20 $\mu$ l and the detection wavelength was set to 214 nm which falls in the UV absorption range for the most sensitive detection for polypeptides of all types. The calibration curve of insulin was constructed from insulin stock solution prepared at a range of 0 – 500  $\mu$ g/ml.

### **6.3.3 Determination of the encapsulation efficiencies of microparticles**

The encapsulation efficiency of insulin in the microparticles was determined using an indirect method. Instead of measuring the amount of drug entrapped within the microparticles, this indirect method relied on the free insulin present in the supernatant solution. The encapsulation efficiency was determined by separating the PLGA microparticles from the excess PVA solution containing free insulin. This was done by centrifugation at 4500 rpm for 20 minutes using Beckman Benchtop Centrifuge and supernatant was collected. The amount of drug present in the supernatant was measured using the HPLC procedure described in section 6.3.2 for detection of insulin which was then compared to the responses in the calibration curve. The drug present in the supernatant reflected the amount of unloaded drug which was used in equation 8 to

calculate the amount of encapsulated drug in the microparticle. The encapsulation efficiency of porous and non-porous PLGA microparticles was then compared.

$$EE \% = \frac{(\text{Total insulin in formulation} - \text{Free insulin in supernatant})}{\text{Total insulin in formulation}} \times 100 \dots \dots \dots (8)$$

#### 6.3.4 *In vitro* insulin release studies

The insulin release studies are based upon the modified protocols in a study to determine the relationship between insulin release and glucose selectivity of multiboronic acid-conjugated chitosan scaffolds (Siddiqui *et al.* 2017). The collected insulin loaded microparticles was lyophilised and stored in -20<sup>0</sup>C after freeze drying before further analysis. Insulin loaded PLGA microparticles were studied in a glucose media in order to determine the relationship between glucose absorption capacity of the microparticles and insulin release. Glucose solution was prepared by dissolving 30 mg of glucose in 10 ml of ultra-purified water to produce 3 mg/ml glucose solution. The glucose solution exhibited a pH value of 7 indicating neutrality as glucose does not dissociate to release H<sup>+</sup> or OH<sup>-</sup> ions upon dissolving in the ultra-purified water. Several 10 mg replicas of chitosan coated porous and non-porous microparticle sample were placed in Eppendorf tubes containing 1 ml of glucose solution and incubated at 37<sup>0</sup>C with horizontal shaking at 100 rpm on a WiseCube WIS-20, Precise Shaking Incubator. At set intervals of 10 minutes, one of the Eppendorf tube from each sample was withdrawn and centrifuged at 14000 rpm for 5 minutes using a Beckman Coulter Microfuge 16 centrifuge. The collected supernatant was then injected to the HPLC system. The amount of insulin released from the PLGA microparticles was determined by comparing the peak area

obtained with those in the calibration curve. The same procedure was repeated for 6 intervals with each withdrawn tube being discarded after centrifugation. Each measurement was done in triplicates.

## 6.4 Results and Discussion

### 6.4.1 HPLC analysis of insulin standard solution

The HPLC system was set up to detect insulin at a wavelength of 214 nm. Figure 25 shows the chromatogram of insulin standard solution at 500  $\mu\text{g/ml}$  after elution for 7 minutes. It can be seen that there is one clearly resolved peak representing the insulin peak at an elution time of approximately 2.6 minutes.

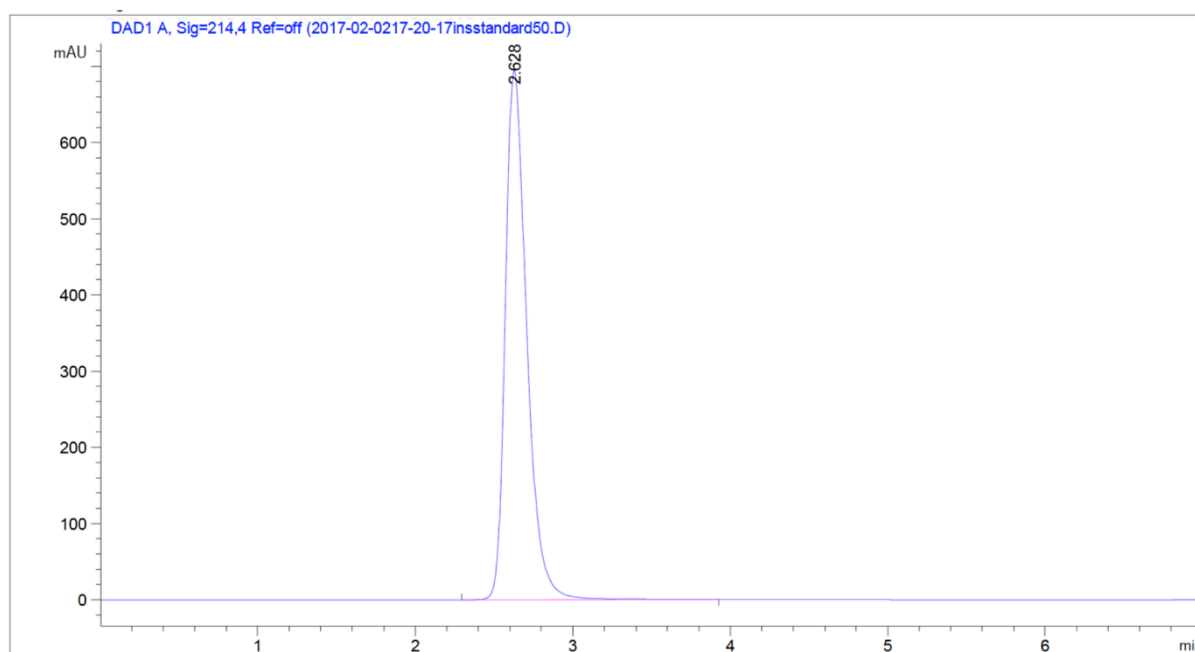


Figure 25: Chromatogram of insulin standard solution 500  $\mu\text{g/ml}$

The calibration curve was constructed from insulin standard solution range of 500 to 0  $\mu\text{g/ml}$ . The calibration curve obtained is presented in Figure 26. The curve was constructed by plotting the peak area with insulin concentration. It can be seen from the figure that the responses (peak area) are proportional to the insulin concentration which with a good linearity reflected by the coefficient of determination ( $R^2$ ) value of 0.999.

The standard curve was used to determine both the encapsulation efficiency of the microparticles as well as the insulin release profile of the samples.

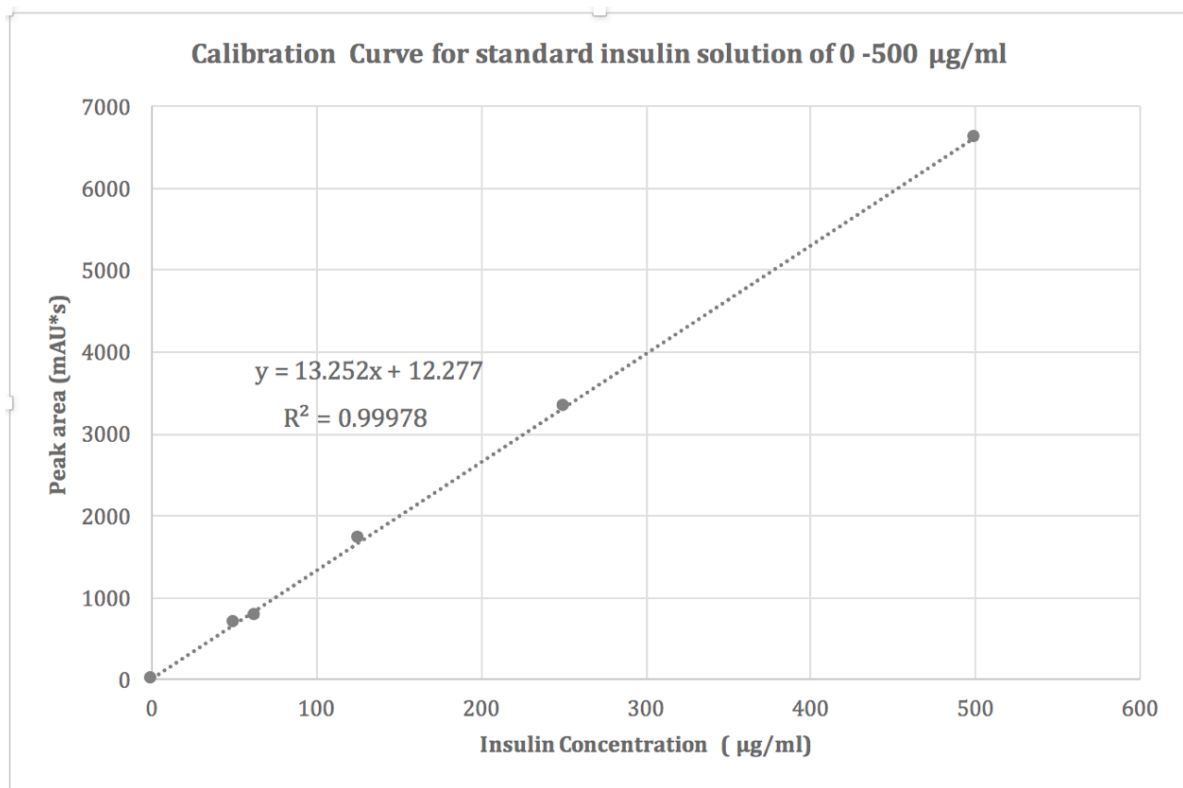


Figure 26: Calibration curve for insulin standard solution 0 - 500 µg/ml

#### 6.4.2 Encapsulation efficiencies of porous and non-porous insulin loaded PLGA microparticles

Encapsulation efficiency gives an approximate indication of the amount of drug that was successfully entrapped within the PLGA microparticles during formulation. The amount of insulin entrapped in the microparticle sample was determined indirectly by measuring the amount in the supernatant. The encapsulation efficiency of insulin in porous and non-porous PLGA microparticles is shown in Figure 27.

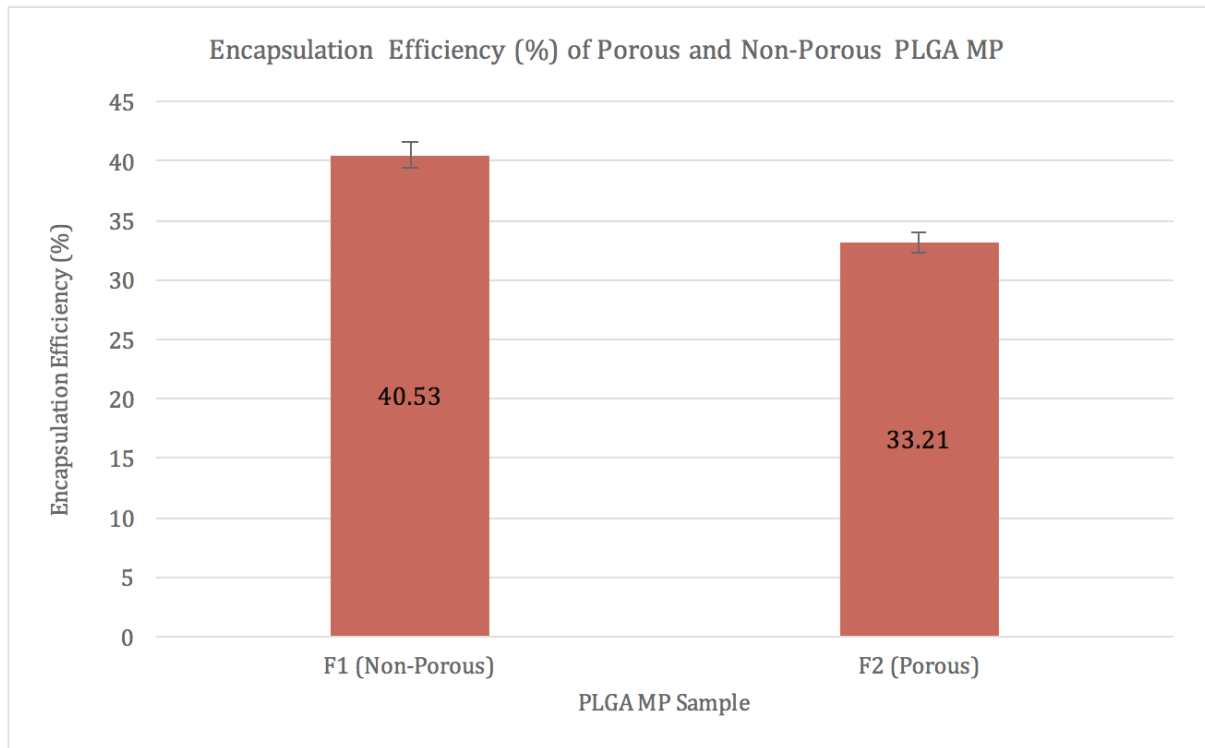


Figure 27: Encapsulation efficiency of non-porous and porous PLGA microparticle

The encapsulation of insulin in both samples were relatively lower than reported values for other drugs including lamivudine (Dev *et al.* 2010), budesonide (Oh *et al.* 2011) and lysozyme (Yang *et al.* 2009) used in their PLGA microparticles. This is likely due to the method used for the incorporation of insulin into the microparticle formulation in the present investigation. As insulin is only partially soluble in water, 0.01M acetic acid was used to dissolve it (European Pharmacopoeia Commission 2005). We did not incorporate the insulin solution in the primary emulsion because the low pH due to acetic acid would have reduced the overall negative charge within PLGA. This in would have compromised on the effectiveness of the positively charged 4-FPBA-chitosan interacting with the negatively charged PLGA and hence impact on the amount of 4-FPBA available. Thus, we decided to add insulin to the chitosan solution prior to homogenisation to form the

secondary emulsion with PVA surfactant. With this procedure however, the encapsulation efficiency of the microparticles to insulin was significantly affected by the presence of insulin in the aqueous phase. A significant amount of insulin may have leaked out of the microparticles to the PVA solution during the formation of the secondary emulsion and hardening process.

The amount of chitosan in the formulation may potentially have also contributed to a decrease in the encapsulation efficiency for insulin (Wang *et al.* 2013). This is because of the mutual attraction between the positively charged chitosan and the negatively charged insulin so that the amount of insulin incorporated within the microparticles was also dependant on the amount of chitosan incorporated (Koppolu 2015). This assertion is substantiated by Wang *et al.* (2013) who found that a higher chitosan concentration increased the likelihood of interaction between anionic proteins and cationic chitosan molecules prior to particle formation (Wang *et al.* 2013). Furthermore, the same authors also postulated that this protein-chitosan binding resulted in lower encapsulation efficiency of the protein in PLGA nanoparticle formulations at the expense of higher chitosan content (Wang *et al.* 2013). Through homogenisation and hardening of the microparticles as well as centrifugation for particle collection, some of the chitosan that contained adsorbed insulin may not have coated unto the surface of the microparticle and leaked out to the PVA solution which further decreased the encapsulation efficiency.

Figure 27 shows that the encapsulation efficiency of non-porous PLGA microparticles was approximately 7% higher than the porous sample. The porous structure on the surface of the microparticle allowed some of the insulin entrapped within to easily leach out (Ilyas *et al.* 2013). Conversely, in the non-porous PLGA microparticles the encapsulated insulin was largely retained subsequent to formulation.

### 6.4.3 In vitro insulin release studies of PLGA microparticles

Insulin release studies for the PLGA microparticles were conducted in glucose solution to determine the relationship between glucose absorption of the PLGA microparticle and insulin release. The glucose solution was set to 3 mg/ml to model the worst case scenario in blood glucose level of diabetic patient. Patients who suffer from diabetes Type 2 have fluctuating blood glucose level with peaks and valleys throughout the day and frequently experience a spike in blood glucose level around 2 hours after a meal with levels reaching 200 mg/dl (2 mg/ml) or more (Diabetes UK 2017). In contrast, non-diabetics would only see a spike up to 140 mg/dl (1.4 mg/ml) after a meal (Diabetes UK 2017). With a relatively high glucose concentration, an in-vitro insulin release study would be vital in helping us decipher the performance of the porous and non-porous microparticles in severely high blood glucose level experienced by some diabetics. A faster response time reflected by a higher insulin release profile shows a higher sensitivity towards glucose. Figure 28 shows the insulin release profile for porous and non-porous PLGA microparticle samples.

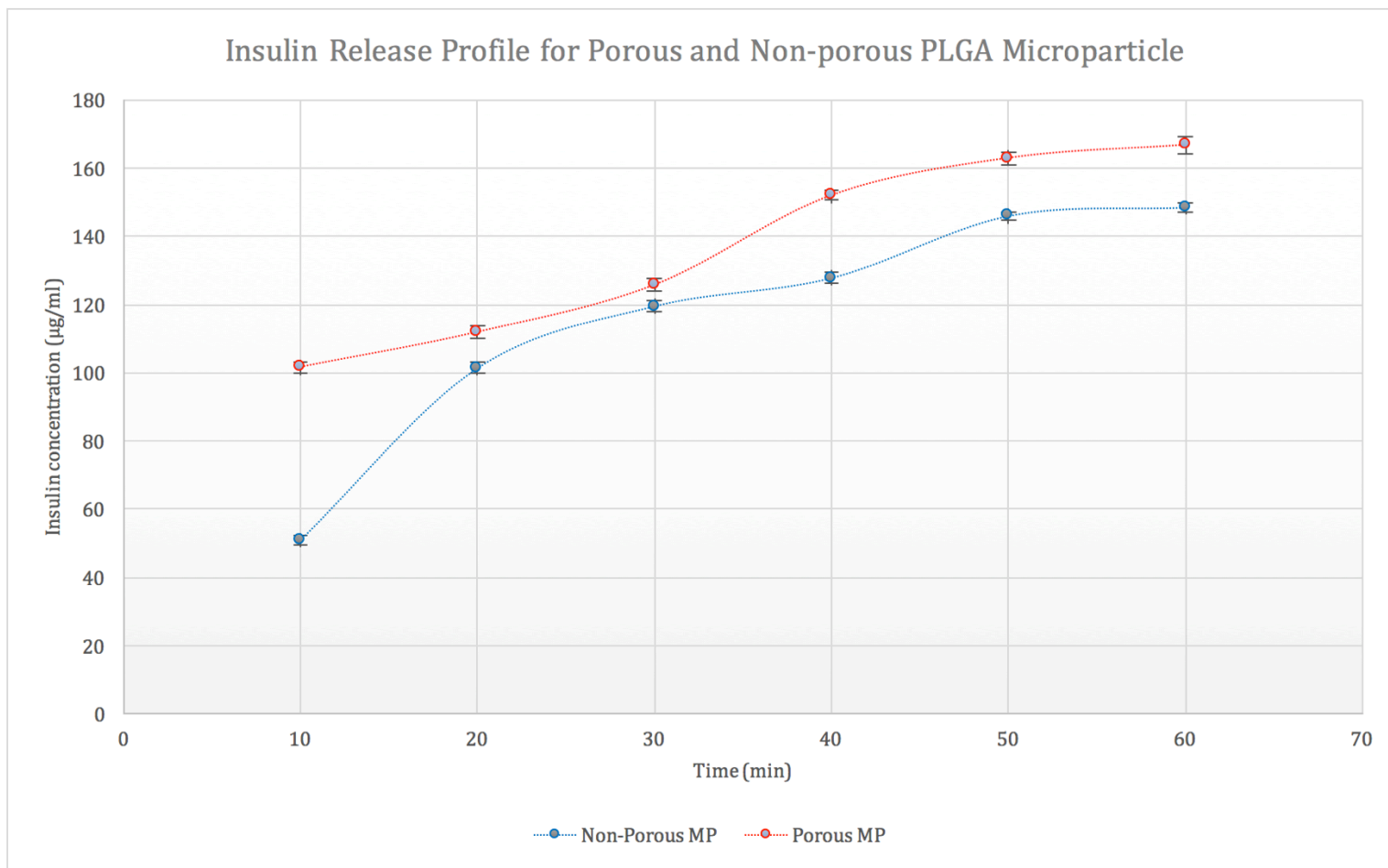


Figure 28 : Insulin release profile for porous and non-porous PLGA microparticle formulations

Figure 28 shows that the insulin release profile for porous PLGA microparticle sample was consistently higher as compared to the non-porous sample. The initial insulin release from the porous PLGA microparticles (101.7  $\mu\text{g/ml}$ ) was approximately double that of the non-porous PLGA microparticle sample (50.9  $\mu\text{g/ml}$ ). However, after 20 minutes, the non-porous sample showed a drastic burst of insulin release (101.3  $\mu\text{g/ml}$ ) while the porous sample showed a more sustained release rate but retained a higher rate (111.9  $\mu\text{g/ml}$ ) during that interval. Over the next 40 minutes, there was no further drastic release in both samples and the observed trend continued with a higher insulin release exhibited by the porous chitosan PLGA microparticles. The higher insulin release profile exhibited by the porous chitosan PLGA microparticles was primary due to the higher 4-FPBA content as presumed earlier. In aqueous systems, the boronic acid moieties in 4-FPBA exists in equilibrium with the neutral trigonal form (1) and the dissociated anionic tetrahedral form (2). The aqueous boronic acid moieties forms reversible and stable covalent complexes with 1,2 -diols or 1,3 -diols in glucose as shown in Figure 29 (Jennifer N. Cambre & Sumerlin 2011). The conversion of neutral boronic acid moieties to anionic cyclic boronate ester (3) causes a change in the hydrophilicity of the overall polymer. This transition from neutral, hydrophobic PLGA polymer to a more hydrophilic polyanion results in the glucose swelling behaviour which is the precursor to insulin release (Jennifer N. Cambre & Sumerlin 2011; Guan & Zhang 2013). As the concentration of boronic acid moiety increases in the system, the ratio of anionic boronate to boronate ester also increases with respect to neutral boronic acid moieties in the presence of the same diols resulting in a higher degree of change in the hydrophilicity of the polymer. Thus, the higher 4-FPBA content in the porous PLGA microparticles resulted in an increased swelling behaviour of the particles in response to glucose

solution and subsequently this swelling squeezes out any dislodged insulin which caused an increase in the diffusion rate of insulin from the microparticle. It must be added that the swelling eventually also causes an increase in path length for diffusing by insulin through the polymer network and this tends to slow down the rate of insulin release. This phenomenon seems to be operational after 40 mins when the insulin release appears more sustained.

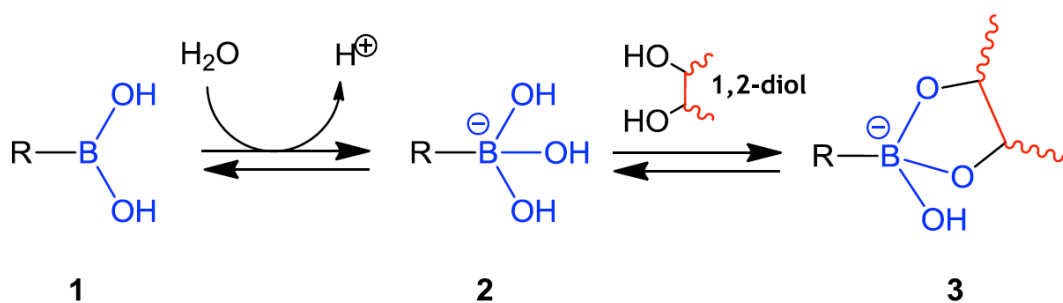


Figure 29: Glucose response behavior of boronic acid moieties

The higher insulin release observed in the porous PLGA microparticles can also be attributed to the inherent porosity of the microparticle. An increased in surface area for drug diffusion and better flow of fluid through a leaky interstitium resulted in a higher insulin release profile observed (Ilyas *et al.* 2013). Thus, a higher insulin release profile can be obtained by increasing the porosity of the microparticle.

## 6.5 Summary

Insulin was successfully encapsulated into the microparticle by adding insulin into the chitosan solution and subsequently, into the PVA solution prior to the formation of the secondary emulsion. Encapsulation efficiency was determined based upon the indirect method of measuring the amount of free insulin in the supernatant. It was found that the encapsulation efficiency of the microparticles was lower than other reported studies and this could be due to the formation of insulin-chitosan which is then dictated by the concentration of chitosan in the microparticles. In addition, incorporating insulin in the secondary aqueous phase caused significant amount of insulin to leak out during particle formation and hardening. Overall, it was found that the encapsulation efficiency of the porous microparticles was lower than non-porous sample as entrapped insulin was more likely to flow out due to the porosity of the microparticle structure.

The insulin release profile of the microparticles in glucose solution showed that higher insulin release was observed for porous PLGA microparticles. This is due to the higher 4-FPBA content in the porous formulation which caused an increase in glucose swelling behaviour of the microparticles and consequently, increased the diffusion rate of insulin from the microparticle. In addition, more insulin was able to flow out due to the better flow of fluid afforded by the porosity of the microparticles. This results show that higher insulin release can be obtained by increasing the porosity and consequently, sensitivity of the PLGA microparticles towards glucose.

## 7.0 CONCLUSIONS AND FUTURE WORK

This study was successful in formulating chitosan coated PLGA microparticles for insulin delivery. The first main objective of this study was to impart glucose sensitivity characteristics to the PLGA microparticle. This was achieved by first conjugating 4-formylphenyl boronic acid (4-FPBA) with chitosan. The successful conjugation of 4-FPBA and chitosan proceed through N-reductive alkylation reaction by utilizing the Schiff's base method. Through analytical methods including FTIR, FESEM and DSC analysis, several key observations were made. Through FTIR, it was found that the boronic acid moiety was bonded to the reactive primary amine site of the chitosan backbone. Furthermore, DSC analysis revealed that an increase in the degree of substitution in the conjugates was correlated to the consumption of the  $-NH_2$  group which provides a viable avenue for formulating conjugates with high amount of boronic acid content. Basically, by increasing the amount of 4-FPBA in the reaction, the resulting conjugates tends towards emulating the physical properties of pure 4-FPBA more than that of pure chitosan suggesting the physical properties of the conjugates were modified. This was further confirmed with FESEM imaging and showed that conjugated chitosan with high amount of boronic acid moieties were able to be formulated with relative ease. With the successful formulation of conjugated chitosan, the second objective of this study was to formulate porous and non-porous PLGA microparticles with chitosan coating. Double emulsion method was used to formulate the microparticles with modifications to incorporate the modified chitosan. Phosphate buffer saline (PBS) was used as a porogen to induce porosity to the microparticles and subsequent exposure to ethanolic- NaOH was done to enhance porosity. Through FESEM imaging, the formulated non-porous microparticles formulation showed spherical microparticles of relatively uniform sizes in

the range of 1.0 to 10.0  $\mu\text{m}$  with no agglomeration. After porosity optimisation by adjusting the concentration of ethanolic  $\text{-NaOH}$ , the porous formulation obtained were spherical, stable with numerous pores observed on the surface.

Glucose absorption of the PLGA microparticles was done through an indirect method utilising curcumin to detect 4-FPBA content in the microparticle samples. Higher amount of 4-FPBA correlates to a higher glucose sensitivity of the microparticles as observed in the insulin release studies. From HPLC analysis, the percentage of curcumin consumed by the porous PLGA microparticles was higher than the non-porous formulations which suggest that the increased in surface area afforded by the porous PLGA microparticle caused more of the modified chitosan to be incorporated unto the surface of the particle, thereby allowing a higher amount of 4-FPBA to be readily available for interaction with curcumin.

Insulin release studies were then performed on both porous and non-porous PLGA microparticles to further define the relationship between the amount of insulin release and glucose sensitivity characteristic of the microparticles. From the insulin release profile obtained, porous PLGA microparticles showed a higher insulin release due to the higher amount of 4-FPBA content which caused an increased swelling of the microparticle in glucose solution, thereby releasing more of the insulin payload through diffusion. The more porous microstructure of the PLGA microparticle also played a role and allowed more insulin to flow out due to the better flow of fluid resulting in higher insulin release. Thus, the overall higher insulin release profile obtained for porous PLGA microparticle sample was achieved due to the higher glucose absorption characteristic afforded by high amount of 4-FPBA available as well as the porous microstructure afforded by the microparticle.

While all the objectives of this study were fulfilled, a number of issues remained that require further investigation. Low encapsulation efficiency of insulin presents a complication with the microparticles as high drug encapsulation is generally preferred to ensure viability of the PLGA microparticles in drug delivery applications. High encapsulation efficiency results in fewer microparticles needed to deliver the required dosage to the patient. Furthermore, a more comprehensive insulin release study is required to fully model the drug release profile of both types of microparticles. Drug loaded PLGA microparticles are known for having an initial burst release profile with a more sustained release after a few days. Burst release can then be enhanced or suppressed depending on the objective by tuning specific parameters in the formulation. Thus, the new study should model the drug release over a prolonged amount of time to fully describe the drug release rate of the microparticles.

## 8.0 REFERENCES

- Abdel-Magid, A.F. et al., 1996. Reductive Amination of Aldehydes and Ketones with Sodium Triacetoxyborohydride. Studies on Direct and Indirect Reductive Amination Procedures1. *The Journal of Organic Chemistry*, 61(11), pp.3849–3862. Available at: <http://dx.doi.org/10.1021/jo960057x>.
- American Diabetes, A., 2012. Standards of Medical Care in Diabetes—2013. *Diabetes Care*, 36(Supplement 1), p.S11 LP-S66. Available at: [http://care.diabetesjournals.org/content/36/Supplement\\_1/S11.abstract](http://care.diabetesjournals.org/content/36/Supplement_1/S11.abstract).
- American Diabetes, A., 2013. Standards of Medical Care in Diabetes—2014. *Diabetes Care*, 37(Supplement 1), p.S14 LP-S80. Available at: [http://care.diabetesjournals.org/content/37/Supplement\\_1/S14.abstract](http://care.diabetesjournals.org/content/37/Supplement_1/S14.abstract).
- Arayne, M.S. & Sultana, N., 2006. Porous nanoparticles in drug delivery systems. *Pak J Pharm Sci*, 19(October), pp.158–169. Available at: <http://www.ncbi.nlm.nih.gov/pubmed/16751130>.
- Asantewaa, Y. et al., 2013. Correlating Physicochemical Properties of Boronic Acid-Chitosan Conjugates to Glucose Adsorption Sensitivity. *Pharmaceutics*, 5(1), pp.69–80.
- Birnbaum, D.T., Kosmala, J.D. & Brannon-peppas, L., 2000. Optimization of preparation techniques for poly ( lactic acid-co-glycolic acid ) nanoparticles. *Nanoparticle Research*, 2(2), pp.173–181.
- Blaine, R.L., 2015. Determination of Polymer Crystallinity by DSC. *TA Instruments*, pp.1–3. Available at: <http://www.tainstruments.com/pdf/literature/TA123new.pdf> [Accessed March 7, 2017].
- Brooks, W.L.A. & Sumerlin, B.S., 2015. Synthesis and Applications of Boronic Acid-Containing Polymers: From Materials to Medicine. *Chemical Reviews*, p.150914115935000. Available at: <http://pubs.acs.org/doi/10.1021/acs.chemrev.5b00300>.
- Cambre, J.N. & Sumerlin, B.S., 2011. Biomedical applications of boronic acid polymers. *Polymer*, 52(21), pp.4631–4643. Available at: <http://linkinghub.elsevier.com/retrieve/pii/S0032386111006495>.
- Cambre, J.N. & Sumerlin, B.S., 2011. Biomedical applications of boronic acid polymers. *Polymer*, 52(21), pp.4631–4643. Available at: <http://www.sciencedirect.com/science/article/pii/S0032386111006495>.
- Carino, G.P., Jacob, J.S. & Mathiowitz, E., 2000. Nanosphere based oral insulin delivery. *Journal of Controlled Release*, 65(1–2), pp.261–269. Available at: <http://www.sciencedirect.com/science/article/pii/S0168365999002473>.

- Carr, D., 2016. A Guide to the Analysis and Purification of Proteins and Peptides by Reversed-Phase HPLC.
- Chakraborty, C. et al., 2011. Landscape Mapping of Functional Proteins in Insulin Signal Transduction and Insulin Resistance: A Network-Based Protein-Protein Interaction Analysis. *PLOS ONE*, 6(1), p.e16388. Available at: <http://dx.doi.org/10.1371/journal.pone.0016388>.
- Chiranjib, C. et al., 2013. Nanoparticles as “smart” pharmaceutical delivery. *Frontiers in Bioscience*, 18, pp.1030–1050.
- Crotts, G. & Park, T.G., 1998. Protein delivery from poly(lactic-co-glycolic acid) biodegradable microspheres: Release kinetics and stability issues. *Journal of Microencapsulation*, 15(6), pp.699–713. Available at: <http://dx.doi.org/10.3109/02652049809008253>.
- De, S. & Robinson, D.H., 2004. Particle Size and Temperature Effect on the Physical Stability of PLGA Nanospheres and Microspheres Containing Bodipy. *AAPS PharmSciTech*, 5(4), pp.1–7.
- Dev, A. et al., 2010. Preparation of poly(lactic acid)/chitosan nanoparticles for anti-HIV drug delivery applications. *Carbohydrate Polymers*, 80(3), pp.833–838. Available at: <http://www.sciencedirect.com/science/article/pii/S0144861710000020>.
- Diabetes UK, 2017. Blood Sugar Level Ranges. Available at: [http://www.diabetes.co.uk/diabetes\\_care/blood-sugar-level-ranges.html](http://www.diabetes.co.uk/diabetes_care/blood-sugar-level-ranges.html) [Accessed April 20, 2017].
- Ding, W. et al., 2003. Synthesis and characterization of a novel derivative of chitosan. *Polymer*, 44(3), pp.547–556.
- European Pharmacopoeia Commission, 2005. INSULIN , HUMAN Insulinum humanum. In *EUROPEAN PHARMACOPOEIA*. pp. 1800–1802. Available at: <http://www.uspbpep.com/ep50/Insulin, human.pdf>.
- Fan, L. & Singh, S.K., 1989. *Controlled Release: A Quantitative Treatment*,
- Fogler, H.S., 2006. *Elements of chemical reaction engineering*,
- Galant, A.L., Kaufman, R.C. & Wilson, J.D., 2015. Glucose : Detection and analysis q. *Food Chemistry*, 188, pp.149–160. Available at: <http://dx.doi.org/10.1016/j.foodchem.2015.04.071>.
- Guan, Y. & Zhang, Y., 2013. Boronic acid-containing hydrogels: synthesis and their applications. *Chemical Society Reviews*, 42(20), p.8106. Available at: <http://xlink.rsc.org/?DOI=c3cs60152h>.
- Guo, C. & Gemeinhart, R.A., 2008. Understanding the adsorption mechanism of chitosan onto poly(lactide-co-glycolide) particles. *European Journal of Pharmaceutics and Biopharmaceutics*, 70(2), pp.597–604. Available at: <http://www.sciencedirect.com/science/article/pii/S0939641108002233>.
- Hall, D.G., 2011. Structure , Properties , and Preparation of Boronic Acid Derivatives Overview of Their Reactions and Applications.

- Hall, J.B. et al., 2007. Characterization of nanoparticles for therapeutics. *Nanomedicine*, 2(6), pp.789–803. Available at: <http://dx.doi.org/10.2217/17435889.2.6.789>.
- Hirenkumar, M. & Siegel, S., 2012. PLGA as Biodegradable Drug Delivery Carrier. *Polymers*, 3(3), pp.1–19.
- Ilyas, A. et al., 2013. Salt-leaching synthesis of porous PLGA nanoparticles. *IEEE Transactions on Nanotechnology*, 12(6), pp.1082–1088.
- Kittur, F.S. et al., 2002. Characterization of chitin, chitosan and their carboxymethyl derivatives by differential scanning calorimetry. *Carbohydrate Polymers*, 49(2), pp.185–193. Available at: <http://www.sciencedirect.com/science/article/pii/S0144861701003204>.
- Klose, D. et al., 2006. How porosity and size affect the drug release mechanisms from PLGA-based microparticles. *International Journal of Pharmaceutics*, 314(2), pp.198–206.
- Koppolu, B. prasanth, 2015. Controlling chitosan-based encapsulation for protein and vaccine delivery. , 35(14), pp.4382–4389.
- Kumari, A., Yadav, S.K. & Yadav, S.C., 2010. Biodegradable polymeric nanoparticles based drug delivery systems. *Colloids and Surfaces B: Biointerfaces*, 75(1), pp.1–18. Available at: <http://www.sciencedirect.com/science/article/pii/S0927776509004111>.
- Lawrence, K. et al., 2012. Analytical Methods COMMUNICATION A simple and effective colorimetric technique for the detection of boronic acids and their derivatives †. , pp.2215–2217.
- Liu, J. et al., 2007. Controlled release of insulin from PLGA nanoparticles embedded within PVA hydrogels. *Journal of Materials Science: Materials in Medicine*, 18(11), pp.2205–2210. Available at: <http://dx.doi.org/10.1007/s10856-007-3010-0>.
- Lowman, A.M. et al., 2016. Oral delivery of insulin using pH-responsive complexation gels. *Journal of Pharmaceutical Sciences*, 88(9), pp.933–937. Available at: <http://dx.doi.org/10.1021/js980337n>.
- Luan, X. et al., 2006. Key parameters affecting the initial release (burst) and encapsulation efficiency of peptide-containing poly(lactide-co-glycolide) microparticles. *International Journal of Pharmaceutics*, 324(2), pp.168–175. Available at: <http://www.sciencedirect.com/science/article/pii/S0378517306004546>.
- Matsumoto, M., Shimizu, T. & Kondo, K., 2002. Selective adsorption of glucose on novel chitosan gel modified by phenylboronate. *Separation and Purification Technology*, 29(3), pp.229–233. Available at: <http://www.sciencedirect.com/science/article/pii/S1383586602000850>.
- Murakami, H. et al., 1997. Influence of the degrees of hydrolyzation and polymerization of poly(vinylalcohol) on the preparation and properties of poly(dl-lactide-co-glycolide) nanoparticle. *International Journal of Pharmaceutics*, 149(1), pp.43–49. Available at: <http://www.sciencedirect.com/science/article/pii/S0378517396048545>.
- Oh, Y.J. et al., 2011. Preparation of budesonide-loaded porous PLGA microparticles and

- their therapeutic efficacy in a murine asthma model. *Journal of Controlled Release*, 150(1), pp.56–62. Available at:  
<http://www.sciencedirect.com/science/article/pii/S0168365910008990>.
- Owens, D.R., Zinman, B. & Bolli, G.B., 2016. Insulins today and beyond. *The Lancet*, 358(9283), pp.739–746. Available at: [http://dx.doi.org/10.1016/S0140-6736\(01\)05842-1](http://dx.doi.org/10.1016/S0140-6736(01)05842-1).
- Polysciences, I., 2016. *PLGA (Poly Lactic co- Glycolic Acid) Uniform Dry Microsphere*, Available at:  
[http://www.polysciences.com/skin/frontend/default/polysciences/pdf/TDS\\_858.pdf](http://www.polysciences.com/skin/frontend/default/polysciences/pdf/TDS_858.pdf).
- Qutachi, O. et al., 2014. Injectable and porous PLGA microspheres that form highly porous scaffolds at body temperature. *Acta Biomaterialia*, 10(12), pp.5090–5098. Available at: <http://www.sciencedirect.com/science/article/pii/S1742706114003511>.
- Sahoo, S.K. et al., 2002. Residual polyvinyl alcohol associated with poly (d,l-lactide-co-glycolide) nanoparticles affects their physical properties and cellular uptake. *Journal of Controlled Release*, 82(1), pp.105–114. Available at:  
<http://www.sciencedirect.com/science/article/pii/S016836590200127X>.
- Santucci, L. & Gilman, H., 1958. Some Bromine-containing and Sulfur-containing Aromatic Boronic Acids. *Journal of the American Chemical Society*, 80(1), pp.193–196. Available at: <http://dx.doi.org/10.1021/ja01534a048>.
- Sharma, G. et al., 2015. Nanoparticle based insulin delivery system : the next generation efficient therapy for Type 1 diabetes. *Journal of Nanobiotechnology*, pp.1–13.
- Shrivastava, A. & Gupta, V., 2011. Methods for the determination of limit of detection and limit of quantitation of the analytical methods. *Chronicles Young Scientist*, 2(1), pp.21–25.
- Siddiqui, N.A., Billa, N. & Roberts, C.J., 2017. Multiboronic acid-conjugated chitosan scaffolds with glucose selectivity to insulin release. *Journal of Biomaterials Science, Polymer Edition*, 5063(March), p.0. Available at:  
<http://dx.doi.org/10.1080/09205063.2017.1301774>.
- Siepmann, J. et al., 2005. How Autocatalysis Accelerates Drug Release from PLGA-Based Microparticles: A Quantitative Treatment. *Biomacromolecules*, 6(4), pp.2312–2319. Available at: <http://dx.doi.org/10.1021/bm050228k>.
- Singh, M.N. et al., 2017. Microencapsulation : A promising technique for controlled drug delivery. , 5(2), pp.65–77.
- Singh, R. & Lillard Jr., J.W., 2009. Nanoparticle-based targeted drug delivery. *Experimental and Molecular Pathology*, 86(3), pp.215–223. Available at:  
<http://www.sciencedirect.com/science/article/pii/S001448000800141X>.
- Smoum, R., Rubinstein, A. & Srebnik, M., 2006. Chitosan–Pentaglycine–Phenylboronic Acid Conjugate: A Potential Colon-Specific Platform for Calcitonin. *Bioconjugate Chemistry*, 17(4), pp.1000–1007. Available at: <http://dx.doi.org/10.1021/bc050357y>.
- Sun, S. et al., 2010. Insulin-S.O (sodium oleate) complex-loaded PLGA nanoparticles: Formulation, characterization and in vivo evaluation. *Journal of*

*Microencapsulation*, 27(6), pp.471–478. Available at:  
<http://dx.doi.org/10.3109/02652040903515490>.

Wang, Y., Li, P. & Kong, L., 2013. Chitosan-Modified PLGA Nanoparticles with Versatile Surface for Improved Drug Delivery. *AAPS PharmSciTech*, 14(2), pp.585–592. Available at: <http://dx.doi.org/10.1208/s12249-013-9943-3>.

Wang, Z.H. et al., 2010. Trimethylated chitosan-conjugated PLGA nanoparticles for the delivery of drugs to the brain. *Biomaterials*, 31(5), pp.908–915. Available at: <http://www.sciencedirect.com/science/article/pii/S0142961209010722>.

Webb, P.A., 2001. Volume and Density Determinations for Particle Technologists. , (February).

Wu, J. et al., 2017. Insulin-loaded PLGA microspheres for glucose- responsive release. *Drug Delivery*, 24(1), pp.1513–1525.

Yang, Y. et al., 2009. Biomaterials Development of highly porous large PLGA microparticles for pulmonary drug delivery. *Biomaterials*, 30(10), pp.1947–1953. Available at: <http://dx.doi.org/10.1016/j.biomaterials.2008.12.044>.

Zhang, X. et al., 2012. Preparation and characterization of insulin-loaded bioadhesive PLGA nanoparticles for oral administration. *European Journal of Pharmaceutical Sciences*, 45(5), pp.632–638. Available at: <http://linkinghub.elsevier.com/retrieve/pii/S0928098712000255>.

## 9.0 APPENDICES

### 9.1 FTIR spectra for formulations F2, F4 and F6 compared to pure PBA and pure chitosan.

